

Alkali Salts of C_3 -Symmetric, Linked Aryloxides: Selective Binding of Substrates with Metal Aggregates

Maarten B. Dinger and Michael J. Scott*[†]

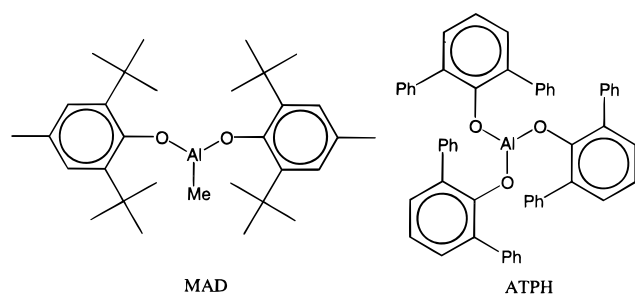
Department of Chemistry, University of Florida, P.O. Box 117200, Gainesville, Florida 32611-7200

Received November 9, 1999

The lithium, sodium, and potassium salts of tris(3,5-dialkyl-2-hydroxyphenyl)methanes (*tert*-butyl, *tert*-pentyl, methyl) have been prepared by reaction of the triarylmethane with *n*-butyllithium, sodium hydride, and potassium hydride, respectively. These compounds are all hexanuclear aggregates composed of two triarylmethane units. Whereas the lithium salt is compact and cannot bind oxygen-donor solvent molecules, the sodium and potassium systems have vacant coordination sites that can interact with solvents. For the sodium compounds, the solvent can be subsequently removed, and the resulting coordinatively unsaturated compounds have been shown to selectively bind oxygen-donor substrates (ethers, aldehydes, and ketones) of suitable size and shape. The paper reports the synthesis and characterization of these novel compounds, including thirteen crystal structures of the salts and their adducts.

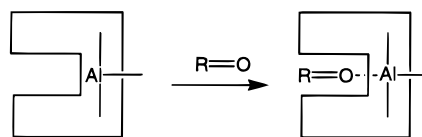
Introduction

Host–guest Lewis acid based compounds¹ and catalysts have become an essential component in many chemical reactions, and, of this class of materials, aluminum complexes ligated by aryloxy groups are especially useful for synthetic applications.² Due to their exceptional properties, two aluminum compounds in particular have garnered much attention, MAD [methylaluminum bis(2,6-di-*tert*-butylphenoxide)]³ and ATPH [aluminum tris(2,6-diphenylphenoxide)].⁴ With substrates containing a



carbonyl functionality, these catalysts will induce numerous stereo-, regio-, and chemoselective carbon–carbon bond forming reactions, among them stereochemically controlled ene reactions of δ,ϵ -unsaturated aldehydes,⁵ exo-selective Diels–Alder reactions,⁶ stereoselective and asymmetric Claisen rearrangements,⁷ stereospecific methylacrylate polymerizations,⁸ and selective

Scheme 1



alkylation of unsymmetrical ketones.³ By providing a sterically crowded environment around the carbonyl group (Scheme 1), the random approach of a second reactant is blocked, inducing specificity in the reaction. In some cases, the carbonyl group is rendered almost inert with respect to other functionalities in the molecule, and the aluminum reagents can act as protecting groups for selective alkylations⁹ and additions to α,β -unsaturated carbonyl compounds (Michael additions).¹⁰ An additional application for these sterically crowded Lewis acids is that they impart molecular recognition properties, and it has been shown that they can discriminate between ethers,¹¹ aldehydes,¹² ketones,¹³ and esters,¹⁴ of differing size and shape.

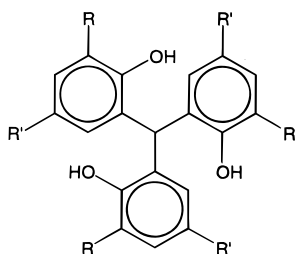
[†] Fax: 352-392-3255. E-mail: mjscott@chem.ufl.edu.

- (1) Vaugois, J.; Simard, M.; Wuest, J. D. *Coord. Chem. Rev.* **1995**, *145*, 55.
- (2) Saito, S.; Yamamoto, H. *Chem. Commun.* **1997**, 1585.
- (3) (a) Maruoka, K.; Itoh, Y.; Sakurai, M.; Nonoshita, K.; Yamamoto, H. *J. Am. Chem. Soc.* **1988**, *110*, 3588. (b) Power, M. B.; Bott, S. G.; Atwood, J. L.; Barron, A. R. *J. Am. Chem. Soc.* **1990**, *112*, 3446.
- (4) Maruoka, K.; Imoto, H.; Saito, S.; Yamamoto, H. *J. Am. Chem. Soc.* **1994**, *116*, 4131.
- (5) Maruoka, K.; Ooi, T.; Yamamoto, H. *J. Am. Chem. Soc.* **1990**, *112*, 9011.
- (6) Maruoka, K.; Imoto, H.; Yamamoto, H. *J. Am. Chem. Soc.* **1994**, *116*, 12115.

- (7) (a) Nonoshita, K.; Banno, H.; Maruoka, K.; Yamamoto, H. *J. Am. Chem. Soc.* **1990**, *112*, 316. (b) Maruoka, K.; Banno, H.; Yamamoto, H. *Tetrahedron: Asymmetry* **1991**, *2*, 647. (c) Nonoshita, K.; Maruoka, K.; Yamamoto, H. *Bull. Chem. Soc. Jpn.* **1992**, *65*, 541. (d) Maruoka, K.; Concepcion, A. B.; Yamamoto, H. *Bull. Chem. Soc. Jpn.* **1992**, *65*, 3501. (e) Maruoka, K.; Saito, S.; Yamamoto, H. *J. Am. Chem. Soc.* **1995**, *117*, 1165. (f) Saito, S.; Shimada, K.; Yamamoto, H. *Synlett* **1996**, 720.
- (8) Kitayama, T.; Hirano, T.; Hatada, K. *Tetrahedron* **1997**, *53*, 15263.
- (9) Ooi, T.; Kondo, Y.; Maruoka, K. *Angew. Chem., Int. Ed.* **1998**, *37*, 3039.
- (10) (a) Childs, R. F.; Mulholland, D. L.; Nixon, A. *Can J. Chem.* **1982**, *60*, 801. (b) Saito, S.; Shimada, I.; Takamori, Y.; Tanaka, M.; Maruoka, K.; Yamamoto, H. *Bull. Chem. Soc. Jpn.* **1997**, *70*, 1671.
- (11) Maruoka, K.; Nagahara, S.; Yamamoto, H. *J. Am. Chem. Soc.* **1990**, *112*, 6115.
- (12) (a) Maruoka, K.; Saito, S.; Yamamoto, H. *Synlett* **1994**, 439. (b) Maruoka, K.; Saito, S.; Concepcion, A. B.; Yamamoto, H. *J. Am. Chem. Soc.* **1993**, *115*, 1183.
- (13) Maruoka, K.; Araki, Y.; Yamamoto, H. *J. Am. Chem. Soc.* **1988**, *110*, 2650.
- (14) (a) Maruoka, K.; Saito, S.; Yamamoto, H. *J. Am. Chem. Soc.* **1992**, *114*, 1089. (b) Maruoka, K.; Imoto, H.; Saito, S.; Yamamoto, H. *Synlett* **1993**, 197.

Although the aluminum materials comprise the vast bulk of the literature concerning Lewis acid systems, a number of other metal systems have also been employed to this end. Catalytic enantioselective Mannich-type reactions for the synthesis of optically active β -amino ketones and esters,¹⁵ among a number of other reactions,¹⁶ have been achieved using zirconium-based systems. Other noteworthy Lewis acid systems derived from lithium phenolates,¹⁷ lanthanum naphtholates,¹⁸ titanium alkoxides,¹⁹ and bis(oxaline)magnesium²⁰ have also been reported.

In the course of our work with the linked aryloxides, tris(3,5-dialkyl-2-hydroxyphenyl)methanes (*tert*-butyl, *tert*-pentyl, methyl) **1a–c**,²¹ the sodium salts of these ligands were found to have a tendency to form Na₆O₆ aggregates, and much like the MAD and ATPH system, the aryloxide groups form a “pocket” around the six metal ions and are able to discriminate molecules on the basis of size and shape.²² Although sodium is not nearly as electrophilic as aluminum, the hazards and expense associated with the alkylaluminum reagents required for the preparation of the aluminum catalysts detract from their synthetic utility, while the sodium complexes of **1a–c** are generated by using relatively innocuous materials, sodium methoxide or sodium hydride. With this in mind, we undertook a detailed investigation into the properties of the sodium aggregates, and herein we report the results of this work, together with research regarding lithium and potassium derivatives.



1a R, R' = *tert*-butyl

1b R, R' = *tert*-pentyl

1c R = *tert*-butyl, R' = methyl

Experimental Section

All manipulations were carried out either in a VAC Nexus drybox or on a vacuum line using standard Schlenk techniques. All solvents used were dried and distilled prior to use. The aldehydes and ketones were used as received from Aldrich, with the exception of pivalophenone (α,α,α -trimethylacetophenone), which was purchased from Lancaster. NMR spectra were recorded on a Varian VXR 300 MHz spectrometer at 299.95 and 75.47 MHz for the proton and carbon channels, respectively, using C₆D₆ solvent, unless otherwise stated. IR spectra were recorded as KBr disks on a Bruker Vector 22 instrument at a resolution of 4 cm⁻¹. UV–vis spectra were recorded on a Varian Cary 50 instrument using diethyl ether as the solvent. The tris(3,5-dialkyl-2-hydroxyphenyl)methanes, **1a–c**, were prepared following reported procedures.²¹

Synthesis of Alkali Salts of 1. 2a. At room temperature, tris(3,5-di-*tert*-butyl-2-hydroxyphenyl)methane (0.200 g, 0.318 mmol) was dissolved in benzene (5 mL) and *n*-butyllithium (1.6 M in hexanes, 0.60 mL, 0.960 mmol) added dropwise. After the evolution of butane had ceased, the flask was stoppered and allowed to stand, and over the course of several hours large, colorless crystals formed. The crystals were filtered off and washed with a small portion of benzene to give **2**·C₆H₆ (0.182 g, 79%). Found: C, 79.7; H, 9.6. Required for C₈₆H₁₂₂O₆·Li₆: C, 79.8; H, 9.5. ¹H NMR: δ 7.56 (s, 6H, ⁴J(H,H) = 2.40 Hz, Ar–H), 7.11 (d, ⁴J(H,H) = 2.40 Hz, 6H, Ar–H), 6.38 (s, 2H, CH), 1.43 (s, 54H, *t*Bu), 1.19 (s, 54H, *t*Bu). ¹³C NMR (75.4 MHz, *d*₈-THF): δ 163.8, 137.5, 135.5, 134.1, 124.5, 119.4 (Ar–C), 42.3 (CH), 36.2, 35.5 [C(CH₃)₃], 32.8, 30.9 [C(CH₃)₃].

3a. Tris(3,5-di-*tert*-butyl-2-hydroxyphenyl)methane (0.051 g, 0.081 mmol) was dissolved in anhydrous ether (20 mL), and dry sodium hydride (0.03 g, excess) was added. The resulting mixture was stirred at room temperature for 17 h. The excess sodium hydride was filtered off, to leave a solution of **3a**, which was sufficiently pure for further reactions. Removal of the solvent left a white residue of tris(3,5-di-*tert*-butylphen-2-olato)methane **3a**. HR–FABMS: calcd for C₈₆H₁₂₂O₆·Na₆ 1388.8628, found 1388.8669. ¹H NMR: δ 8.22 (d, ⁴J(H,H) = 2.40 Hz, 6H, Ar–H), 8.15 (s, 2H, CH), 7.40 (d, ⁴J(H,H) = 2.40 Hz, 6H, Ar–H), 1.50 (s, 54H, *t*Bu), 1.25 (s, 54H, *t*Bu). ¹³C NMR: δ 161.7, 137.2, 134.8, 133.0, 127.4, 121.7 (Ar–C), 35.3, 34.5 [C(CH₃)₃], 32.5 [C(CH₃)₃], 31.6 (CH), 30.7 [C(CH₃)₃].

3b. Tris(3,5-di-*tert*-pentyl-2-hydroxyphenyl)methane (0.252 g, 0.353 mmol) was dissolved in THF (15 mL), and excess sodium hydride was added. The milky solution was refluxed under nitrogen for 1 h. The solvent was evaporated under vacuum, and the resulting dry residue was heated to 80 °C under vacuum for 3 h to remove all coordinated THF. The residue was then dissolved in ether and the excess sodium hydride filtered off, to leave a solution of **3b**, which was sufficiently pure for further reactions. ¹H NMR: δ 7.76 (s, 2H, CH), 7.70 (d, ⁴J(H,H) = 2.40 Hz, 6H, Ar–H), 7.29 (d, ⁴J(H,H) = 2.40 Hz, 6H, Ar–H), 1.76 (q, ³J(H,H) = 7.50 Hz, 12H, CH₂CH₃), 1.70 (q, ³J(H,H) = 7.50 Hz, 12H, CH₂CH₃), 1.39 [s, 36H, C(CH₃)₂], 1.21 [s, 36H, C(CH₃)₂], 0.87 (t, ³J(H,H) = 7.20 Hz, 18H, CH₂CH₃), 0.70 (t, ³J(H,H) = 7.20 Hz, 18H, CH₂CH₃). ¹³C NMR: δ 161.1, 135.0, 133.6, 132.0, 124.4 (Ar–C), 38.5, 37.6 (CH₂CH₃), 37.6, 33.9 [C(CH₃)₂], 33.2 (CH), 29.2, 28.3 [C(CH₃)₂], 9.8, 9.7 (CH₂CH₃).

4a. Tris(3,5-di-*tert*-butyl-2-hydroxyphenyl)methane (0.250 g, 0.079 mmol) was dissolved in THF (5 mL) and excess finely powdered potassium hydride added. The resulting solution was stirred at room temperature overnight. After filtration, the solvent was removed under reduced pressure to leave a slightly off-white powder. Benzene was added, and the suspension was filtered, washed with benzene, and dried under vacuum to give **4a** (0.264 g, 89%). A sample of **4a** was dissolved in THF, and pentane was allowed to diffuse in, to give colorless crystals of **4a**·6THF. The material is only marginally soluble in common deuterated solvents, although ¹H NMR spectra could be obtained in CD₂Cl₂. HR–FABMS: found 1523.652, calcd for C₈₆H₁₂₂O₆K₇ 1523.670 (the material acquires an additional potassium in spectrometer). ¹H NMR (CD₂Cl₂): δ 7.72 (br, 6H, Ar–H), 7.55 (s, br, 2H, CH), 7.06 (br, 6H, Ar–H), 1.30 (s, br, 54H, *t*Bu), 1.27 (s, br, 54H, *t*Bu).

4c. The compound was prepared analogously to **4a** from tris(3-*tert*-butyl-5-methyl-2-hydroxyphenyl)methane (0.101 g, 0.201 mmol) and excess potassium hydride in THF. Workup yielded **4c** as a pure white powder (0.104 g, 84%). With an even lower solubility than **4a**, acquisition of a ¹H NMR spectrum for **4b** was not viable. Found: C, 66.3; H, 7.2. Required for C₆₈H₈₆O₆K₆: C, 66.2; H, 7.0.

Preparation of Adducts of 3. 3a·6THF. Following the procedure described above for the synthesis of **3a**, except using THF as the solvent, slow evaporation led to crystals of **3a**·6THF. The THF molecules were found to be too labile for satisfactory microanalytical data, although X-ray crystallography and ¹H NMR demonstrate the formation of the aggregate. ¹H NMR: δ 8.24 (s, 2H, CH), 8.20 (d, ⁴J(H,H) = 2.40 Hz, 6H, Ar–H), 7.32 (d, ⁴J(H,H) = 2.40 Hz, 6H, Ar–H), 3.33 (m, 24H, THF), 1.53 (s, 54H, *t*Bu), 1.38 (s, 54H, *t*Bu), 1.34 (m, 24H, THF).

3b·6THF. To a C₆D₆ solution of crude **3b** was added 6 equiv of tetrahydrofuran, to give, in situ, the complex **3b**·6THF. ¹H NMR: δ

- (15) Ishitani, H.; Ueno, M.; Kobayashi, S. *J. Am. Chem. Soc.* **1997**, *119*, 7153.
 (16) Hoveyda, A. H.; Morken, J. P. *Angew. Chem., Int. Ed. Engl.* **1996**, *35*, 1262, and references therein.
 (17) Baigrie, L. M.; Seiklay, H. R.; Tidwell, T. T. *J. Am. Chem. Soc.* **1985**, *107*, 5391.
 (18) Gröger, H.; Saida, Y.; Sasai, H.; Yamaguchi, K.; Martens, J.; Shibasaki, M. *J. Am. Chem. Soc.* **1998**, *120*, 3089.
 (19) Manickam, G.; Sundararajan, G. *Tetrahedron: Asymmetry* **1997**, *8*, 2271.
 (20) Carbone, P.; Desimoni, G.; Faita, G.; Filippone, S.; Righetti, P. *Tetrahedron* **1998**, *54*, 6099.
 (21) Dinger, M. B.; Scott, M. J. Submitted for publication.
 (22) Dinger, M. B.; Scott, M. J. *Chem. Commun.* **1999**, 2525.

8.11 (s, 2H, CH), 7.95 (d, $^4J(\text{H,H}) = 2.40$ Hz, 6H, Ar-H), 7.16 (d, $^4J(\text{H,H}) = 2.40$ Hz, 6H, Ar-H), 3.27 (m, 24H, THF), 1.83 (m, 24H, CH_2CH_3), 1.46 [s, 36H, $\text{C}(\text{CH}_3)_2$], 1.38 [s, 36H, $\text{C}(\text{CH}_3)_2$], 1.33 (m, 24H, THF), 0.91 (t, $^3J(\text{H,H}) = 7.20$ Hz, 18H, CH_2CH_3), 0.78 (t, $^3J(\text{H,H}) = 7.20$ Hz, 18H, CH_2CH_3). ^{13}C NMR: δ 162.2, 134.9, 133.3, 132.3, 123.6 (Ar-C), 67.8 (THF), 38.7, 37.6 (CH_2CH_3), 37.6, 34.0 [$\text{C}(\text{CH}_3)_2$], 30.0 (CH), 29.5, 28.7 [$\text{C}(\text{CH}_3)_2$], 25.6 (THF), 9.9, 9.7 (CH_2CH_3).

3b·6CH₂Cl₂ (Dichloromethane). Dry **3b** was dissolved in dichloromethane. Pentane was allowed to diffuse in, depositing colorless blocks of the adduct **3b**·6CH₂Cl₂·2.6CH₂Cl₂ that rapidly lose crystallinity upon removal of the supernatant. ^1H NMR: δ 7.83 (s, 2H, CH), 7.74 (d, $^4J(\text{H,H}) = 2.40$ Hz, 6H, Ar-H), 7.27 (d, $^4J(\text{H,H}) = 2.40$ Hz, 6H, Ar-H), 4.26 (s, 12H, CH_2Cl_2), 1.78 (q, $^3J(\text{H,H}) = 7.50$ Hz, 12H, CH_2CH_3), 1.72 (q, $^3J(\text{H,H}) = 7.50$ Hz, 12H, CH_2CH_3), 1.40 [s, 36H, $\text{C}(\text{CH}_3)_2$], 1.24 [s, 36H, $\text{C}(\text{CH}_3)_2$], 0.88 (t, $^3J(\text{H,H}) = 7.20$ Hz, 18H, CH_2CH_3), 0.71 (t, $^3J(\text{H,H}) = 7.20$ Hz, 18H, CH_2CH_3).

3a·6C₇H₆O (Benzaldehyde). Benzaldehyde (50 μL , 0.492 mmol) was added to an ether solution (15 mL) of crude **3a** (based on 0.100 g of **1a**, 0.080 mmol), resulting in a bright yellow solution. Slow evaporation of the solvent deposited orange crystals, which were washed with pentane to give **3a**·6C₇H₆O (0.142 g, 88%). Found: C, 75.3; H, 8.0. Required for C₈₆H₁₂₂O₆Na₆·6C₇H₆O: C, 75.8; H, 7.9. UV/vis: λ_{max} (ϵ) 368 (995) nm. IR: ν [cm^{-1}] 1712, 1696, 1660 (CO). ^1H NMR: δ 8.88 (6H, s, CHO), 8.63 (s, 2H, CH), 8.13 (d, $^4J(\text{H,H}) = 2.40$ Hz, 6H, Ar-H), 7.37 (12H, d, $^3J(\text{H,H}) = 6.60$ Hz, H-2), 7.32 (d, $^4J(\text{H,H}) = 2.40$ Hz, 6H, Ar-H), 7.01 (12H, t, $^3J(\text{H,H}) = 6.90$ Hz, H-4), 6.95 (12H, t, $^3J(\text{H,H}) = 6.90$ Hz, H-3), 1.52 (s, 54H, *t*Bu), 1.40 (s, 54H, *t*Bu). ^{13}C NMR: δ 193.8 (HCO), 162.6, 137.5 (Ar-C), 136.4 (C-1), 134.2 (C-4), 133.5, 133.0 (Ar-C), 130.1 (C-2), 128.7 (C-3), 127.3, 121.4 (C-Ar), 35.5, 34.4 [$\text{C}(\text{CH}_3)_3$], 32.5 [$\text{C}(\text{CH}_3)_3$], 31.7 (CH), 30.7 [$\text{C}(\text{CH}_3)_3$].

3a·6C₉H₈O (trans-Cinnamaldehyde). Addition of *trans*-cinnamaldehyde (35 μL , 0.278 mmol) to an ether solution of crude **3a** (based on 0.056 g of **1a**, 0.021 mmol) gave an immediate bright orange coloration. Slow evaporation of the ether deposited bright orange crystals, which were washed with pentane to give **3a**·6C₉H₈O (0.058 g, 72%). Found: C, 77.2; H, 8.4. Required for C₈₆H₁₂₂O₆Na₆·6C₉H₈O: C, 77.0; H, 7.9. UV/vis: λ_{max} (ϵ) 393 (1323) nm. IR: ν [cm^{-1}] 1672, 1626 (CO). ^1H NMR: δ 8.79 (d, $^4J(\text{H,H}) = 7.80$, 6H, HCO), 8.59 (s, 2H, CH), 8.12 (d, $^4J(\text{H,H}) = 2.40$ Hz, 6H, Ar-H), 7.37 (d, $^4J(\text{H,H}) = 2.40$ Hz, 6H, Ar-H), 7.11 (m, 12H, Ar-H), 7.01 (m, 18H, Ar-H), 6.83 (d, $^3J(\text{H,H}) = 16.20$ Hz, 6H, PhCH=CH), 6.28 (dd, $^3J(\text{H,H}) = 15.90$ Hz, $^3J(\text{H,H}) = 7.50$ Hz, 6H, PhCH=CH), 1.66 (s, 54H, *t*Bu), 1.53 (s, 54H, *t*Bu). ^{13}C NMR: δ 194.5 (HCO), 162.8 (Ar-C), 152.3 (PhCH=CH), 137.4, 134.5, 133.1, 133.0 (Ar-C), 130.9 (PhCH=CH), 128.9, 128.7, 128.6, 127.4, 121.0 (Ar-C), 35.6, 34.6 [$\text{C}(\text{CH}_3)_3$], 32.8 [$\text{C}(\text{CH}_3)_3$], 31.9 (CH), 30.8 [$\text{C}(\text{CH}_3)_3$].

3a·6C₁₀H₁₄O (Safranal). Addition of safranal (45 μL , 0.300 mmol) to an ether solution of crude **3a** (based on 0.056 g of **1a**, 0.021 mmol) gave an immediate bright yellow coloration. Diffusion of pentane into the ether solution gave bright yellow crystals of **3a**·6C₁₀H₁₄O (0.048 g, 52%). Found: C, 75.9; H, 9.4. Required for C₈₆H₁₂₂O₆Na₆·6C₁₀H₁₄O: C, 76.5; H, 9.1. IR: ν [cm^{-1}] 1656, 1635 (CO). ^1H NMR: δ 9.16 (s, 6H, HCO), 8.44 (s, 2H, CH), 8.06 (s, 6H, Ar-H), 7.25 (s, 6H, Ar-H), 5.69 (pent, 6H, $^3J(\text{H,H}) = 4.50$ Hz, H-4), 5.48 (d, $^3J(\text{H,H}) = 9.00$ Hz, 6H, H-3), 1.80 (s, br, 12H, H-5), 1.61 (s, 18H, Me-2), 1.56 (s, 54H, *t*Bu), 1.51 (s, 54H, *t*Bu), 1.17 (s, 36H, Me-6). ^{13}C NMR: δ 192.1 (HCO), 162.5, 137.6, 137.2, 134.1, 132.9, 129.9, 128.9, 127.0, 121.4 (Ar-C/C=C), 41.1 (Me-2), 35.5, 34.4 [$\text{C}(\text{CH}_3)_3$], 32.8 (C-6), 32.6 [$\text{C}(\text{CH}_3)_3$], 31.6 (CH), 30.8 [$\text{C}(\text{CH}_3)_3$], 26.3 (Me-6), 17.6 (C-5).

3a·6C₈H₁₃O (Cyclohexyl Methyl Ketone). Cyclohexyl methyl ketone (70 μL , 0.509 mmol) was added to an ether solution of **3a** (based on 0.100 g of **1a**, 0.080 mmol). Slow evaporation gave colorless crystals, which were washed with pentane to yield **3a**·6C₈H₁₃O (0.151 g, 89%). Cubes were readily grown by diffusion of pentane into an ether solution of **3a**·6C₈H₁₃O. Found: C, 74.7; H, 9.6. Required for C₈₆H₁₂₂O₆Na₆·6C₈H₁₃O: C, 75.2; H, 9.4. ^1H NMR: δ 8.48 (s, 2H, CH), 8.33 (d, $^4J(\text{H,H}) = 2.40$ Hz, 6H, Ar-H), 7.30 (d, $^4J(\text{H,H}) = 2.40$ Hz, 6H, Ar-H), 1.81 (6H, tt, $^3J(\text{H,H}) = 11.70$ Hz, $^4J(\text{H,H}) = 2.70$ Hz,

H-1), 1.57 (s, 54H, *t*Bu), 1.54–1.48 (15H, m, CH_2), 1.43 (s, 54H, *t*Bu), 1.33 (3H, s, Me), 1.14–0.97 (15H, m, CH_2). ^{13}C NMR: δ 212.3 (CO), 162.4, 137.1, 133.6, 133.2, 127.1, 121.3 (Ar-C), 51.2 (C-1), 35.4, 34.5 [$\text{C}(\text{CH}_3)_3$], 32.7, 31.1 [$\text{C}(\text{CH}_3)_3$], 28.9 (CH), 28.6 (C-2), 27.1 (MeCO), 26.1 (C-4), 25.7 (C-3).

3a·6C₈H₈O (Acetophenone). Acetophenone (60 μL , 0.514 mmol) was added to an ether solution (15 mL) of crude **3a** (based on 0.102 g of **1a**, 0.081 mmol), turning the solution bright yellow. Slow evaporation of the solvent deposited yellow crystals, which were washed with pentane to give **3a**·6C₈H₈O (0.145 g, 85%). Found: C, 76.0; H, 8.0. Required for C₈₆H₁₂₂O₆Na₆·6C₈H₈O: C, 76.2; H, 8.1. IR: ν [cm^{-1}] 1692, 1601, 1584 (CO). ^1H NMR: δ 8.76 (s, 2H, CH), 8.06 (d, $^4J(\text{H,H}) = 2.40$ Hz, 6H, Ar-H), 7.49 (12H, d, $^3J(\text{H,H}) = 6.90$ Hz, H-2), 7.21 (d, $^4J(\text{H,H}) = 2.40$ Hz, 6H, Ar-H), 7.10 (12H, t, $^3J(\text{H,H}) = 6.90$ Hz, H-4), 7.03 (12H, t, $^3J(\text{H,H}) = 6.90$ Hz, H-3), 1.93 (18H, s, MeCO), 1.55 (s, 54H, *t*Bu), 1.35 (s, 54H, *t*Bu). ^{13}C NMR: δ 197.9 (MeCO), 162.7, 137.1 (Ar-C), 136.9 (C-1), 133.0 (Ar-C), 132.8 (C-4), 132.6 (Ar-C), 129.0 (C-2), 128.4 (C-3), 127.6, 121.3 (C-Ar), 35.5, 34.3 [$\text{C}(\text{CH}_3)_3$], 32.4, 31.1 [$\text{C}(\text{CH}_3)_3$], 30.5 (CH), 25.7 (MeCO).

3a·4C₁₁H₁₄O (Pivalophenone). Pivalophenone (80 μL , 0.478 mmol) was added to a solution of **3a** (based on 0.101 g of **1a**, 0.081 mmol). Diffusion of pentane into the solution yielded pale green crystals of **3a**·4C₁₁H₁₄O·2Et₂O (72%). Found: C, 75.1; H, 9.0. Required for C₈₆H₁₂₂O₆Na₆·4C₁₁H₁₄O·2Et₂O: C, 75.8; H, 8.8. IR: ν [cm^{-1}] 1671, 1602 (CO). ^1H NMR: δ 8.25 (d, $^4J(\text{H,H}) = 2.40$ Hz, 6H, Ar-H), 8.19 (s, 2H, CH), 7.61 (8H, d, $^3J(\text{H,H}) = 6.00$ Hz, H-2), 7.40 (d, $^4J(\text{H,H}) = 2.40$ Hz, 6H, Ar-H), 7.08–7.00 (12H, d, H-3,4), 1.49 (s, 54H, *t*Bu), 1.22 (s, 54H, *t*Bu), 1.17 (18H, s, *t*BuCO). ^{13}C NMR: δ 207.3 (*t*BuCO), 161.4, 139.0 (C-1), 137.4, 135.3, 132.6 (Ar-C), 130.7 (C-4), 128.1 (C-2), 127.9 (C-3), 122.1 (Ar-C), 44.0 (*t*BuCO), 35.2, 34.6 [$\text{C}(\text{CH}_3)_3$], 32.4, 30.6 [$\text{C}(\text{CH}_3)_3$], 30.5 (CH), 28.0 (*t*BuCO).

3a·6C₈H₁₄O (2,6-Dimethylcyclohexanone). 2,6-Dimethylcyclohexanone [1 mL (mixture of isomers), 1.38 mmol of trans isomer, 5.96 mmol of cis isomer] was added to an etheral solution (80 mL) of crude **3a** (based on 0.261 g of **1a**, 0.208 mmol). Slow evaporation of the solvent produced colorless crystals, which were thoroughly washed with pentane to give **3a**·6C₈H₁₄O (0.273 g, 65%). Found: C, 74.7; H, 9.7. Required for C₈₆H₁₂₂O₆Na₆·6C₈H₁₄O: C, 75.0; H, 9.7. IR: ν [cm^{-1}] 1713 (CO). ^1H NMR: δ 8.38 (s, 2H, CH), 8.36 (d, $^4J(\text{H,H}) = 2.40$ Hz, 6H, Ar-H), 7.34 (s, $^4J(\text{H,H}) = 2.40$ Hz, 6H, Ar-H), 2.23 (hexet, $^3J(\text{H,H}) = 6.60$ Hz, 10H, H-2 trans isomer), 1.84 (hexet, $^3J(\text{H,H}) = 6.60$ Hz, 2H, H-2 cis isomer), 1.56 (s, 54H, *t*Bu), 1.52–1.44 (m, CH_2), 1.38 (s, 54H, *t*Bu), 1.33–1.10 (m, CH_2), 1.02 (d, $^3J(\text{H,H}) = 6.30$ Hz, 6H, Me cis isomer), 0.88 (d, $^3J(\text{H,H}) = 6.90$ Hz, 30H, Me trans isomer).

3b·6C₉H₁₄O₂ (2,2,6-Trimethylcyclohexane-1,4-dione). 2,2,6-Trimethylcyclohexane-1,4-dione (0.170 g, 0.159 mmol) was added to an ether solution of **3b** (based on 0.252 g of **1b**, 0.177 mmol), without stirring. Colorless crystals of **3b**·6C₉H₁₄O₂·0.4Et₂O were deposited over 24 h (90%). Found: C, 73.3; H, 9.2. Required for C₉₆H₁₄₆O₆Na₆·6C₉H₁₄O₂: C, 73.5; H, 9.3. IR: ν [cm^{-1}] 1721, 1713, 1601 (CO). ^1H NMR: δ 7.94 (s, 2H, CH), 7.78 (d, $^4J(\text{H,H}) = 2.40$ Hz, 6H, Ar-H), 7.25 (d, $^4J(\text{H,H}) = 2.40$ Hz, 6H, Ar-H), 2.25–1.98 (m, 24H, H-3,5), 1.77 (q, $^3J(\text{H,H}) = 7.50$ Hz, 24H, CH_2CH_3), 1.68 (m, 6H, H-3,5), 1.40 [s, 36H, $\text{C}(\text{CH}_3)_2$], 1.28 [s, 36H, $\text{C}(\text{CH}_3)_2$], 0.88 (t, $^3J(\text{H,H}) = 7.20$ Hz, 18H, CH_2CH_3), 0.85 (d, $^3J(\text{H,H}) = 7.20$ Hz, 18H, Me-6), 0.80 (s, 36H, Me-2), 0.73 (t, $^3J(\text{H,H}) = 7.20$ Hz, 18H, CH_2CH_3). ^{13}C NMR: δ 212.3 (C-1), 208.0 (C-4), 161.3, 135.1, 133.3, 132.5, 124.0 (Ar-C), 52.4 (C-3), 44.5 (C-6), 43.7 (C-2), 39.4, (C-5), 38.6 (CH_2CH_3), 37.8 [$\text{C}(\text{CH}_3)_2$], 37.5 (CH_2CH_3), 34.0 [$\text{C}(\text{CH}_3)_2$], 32.1 (CH), 29.1, 28.4 [$\text{C}(\text{CH}_3)_2$], 26.3, 25.5 (Me-2), 14.6 (Me-6), 9.9, 9.8 (CH_2CH_3).

Chemical Separation of Acetophenone and Pivalophenone. To an ether solution of **3a** (based on 0.250 g of **1a**, 0.199 mmol) was added an ether solution of a mixture of acetophenone (140 μL , 1.200 mmol) and pivalophenone (200 μL , 1.196 mmol), turning the solution immediately yellow. The ether was allowed to evaporate, to leave a pale yellow residue. A small quantity of pentane was added and the solid filtered off and washed with additional pentane; NMR and IR spectroscopy revealed the solid as very pure **3a**·6C₈H₈O by comparison with an authentic sample (0.40 g, 95%). The solvent was removed from the supernatant to leave a colorless oil, which NMR analysis showed to be pivalophenone (0.140 g, 72%).

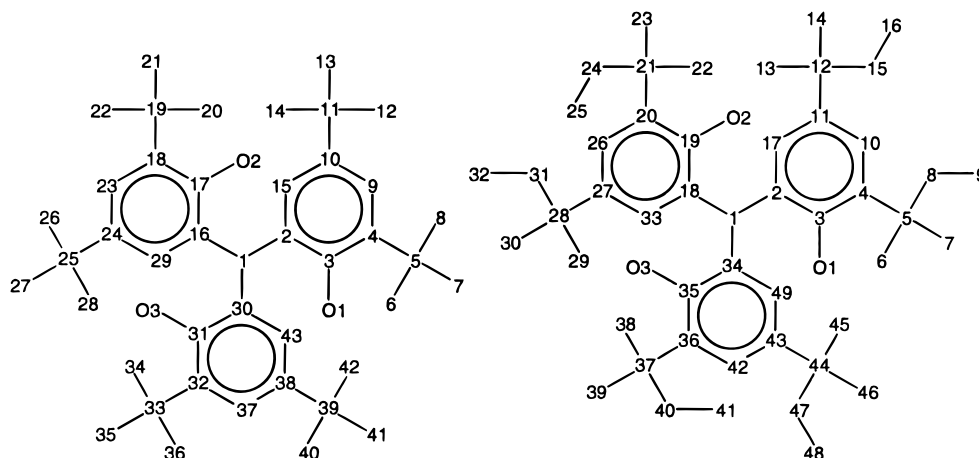


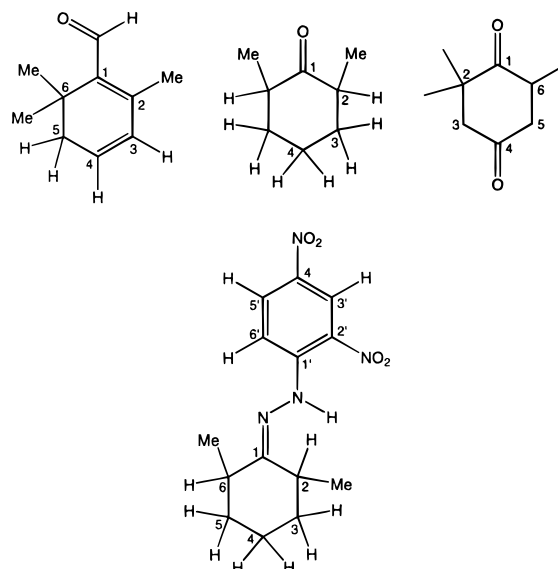
Figure 1. Atom-numbering schemes for the crystal structures derived from **1a** and **1b**, respectively.

Chemical Enrichment of the Trans Isomer of 2,6-Dimethylcyclohexanone. A portion of water (5 mL) was added to an ether solution of **3a**·6C₈H₁₄O, and the resulting ether layer was separated and dried (MgSO₄). An aliquot was injected into a Hewlett-Packard GC equipped with an HP-50+ (50%)-diphenyl (50%)-dimethylsiloxane copolymer) capillary column (30 m, 0.53 mm × 1 μm film thickness) and FID detector. The initial temperature was set to 35 °C, and after injection of the sample, this temperature was maintained for 6.5 min, after which time a temperature ramp of 5 °C/min was used, with the maximum temperature set at 125 °C. Total separation of the isomers was achieved, with the trans isomer showing a retention time of 17.62 min, with the cis isomer at 18.27 min. The ratio of cis:trans isomers of 2,6-dimethylcyclohexanone was integrated and determined to be 16.1:83.9, respectively. The same ratio was determined independently by ¹H NMR spectroscopy from peak integration of the H-2 resonances.

Preparation of Hydrazone Derivative: trans-2,6-Dimethylcyclohexanone 2,4-Dinitrophenylhydrazone. To an ether solution (10 mL) of **3a**·6C₈H₁₄O (0.201 g, 0.094 mmol) was added a concentrated sulfuric acid solution (5 mL) of 2,4-dinitrophenylhydrazine (30 wt % H₂O, 0.160 g, 0.566 mmol), immediately forming a bright orange/yellow solution. Water (30 mL) and ether (10 mL) were both added, and the organic layer was extracted and dried with magnesium sulfate. After filtration, the solvent was removed under reduced pressure to leave a bright orange solid. The material was recrystallized by vapor diffusion of pentane into an ether solution to give *trans*-2,6-dimethylcyclohexanone 2,4-dinitrophenylhydrazone (0.172 g, 73%). Found: C, 54.8; H, 6.0; N, 18.2. Required for C₁₄H₁₈N₄O₄: C, 54.9; H, 5.9; N, 18.3%. ¹H NMR (CDCl₃): δ 11.3 (1H, s, NH), 9.14 (d, 1H, ⁴J(H,H) = 2.70 Hz, H-3'), 8.30 (dd, 1H, ³J(H,H) = 9.90 Hz, ⁴J(H,H) = 2.70 Hz, H-5'), 7.99 (d, 1H, ³J(H,H) = 9.90 Hz, H-6'), 3.15 (m, 1H, H-2), 2.60 (1H, sept, ³J(H,H) = 6.15 Hz, H-2), 2.02 (m, 1H, CH₂), 1.83–1.62 (m, 5H, CH₂), 1.78 (2H, sept, ³J(H,H) = 6.00 Hz, H-3), 1.59 (2H, m, H-4), 1.41 (2H, sept, ³J(H,H) = 6.60 Hz, H-3), 0.94 (6H, d, ³J(H,H) = 7.20 Hz, Me). ¹³C NMR (75.47 MHz, CDCl₃): δ 167.0 (C-1), 35.9 (CH₂), 35.4 (C-6), 32.5 (CH₂), 30.1 (C-2), 20.4 (C-4), 17.1 (Me), 16.7 (Me).

X-ray Crystallography. Unit cell dimensions and intensity data for all of the structures were obtained on a Siemens CCD SMART diffractometer at –100 °C, with the exception of **3a**·5.6C₈H₁₄O·1/2-Et₂O (2,6-dimethylcyclohexanone), which was collected at –125 °C. The data collections nominally covered over a hemisphere of reciprocal space, by a combination of three sets of exposures; each set had a different φ angle for the crystal, and each exposure covered 0.3° in ω. The crystal to detector distance was 5.0 cm. The data sets were corrected empirically for absorption using SADABS.²³

All of the structures were solved using the Bruker SHELXTL software package for the PC, using the direct methods option of SHELXS. The space groups for all of the structures were determined from an examination of the systematic absences in the data, and the successful solution and refinement of the structures confirmed these



assignments. Except for the hydrogens involved in hydrogen-bonding interactions, all hydrogen atoms were assigned idealized locations and were given a thermal parameter equivalent to 1.2 or 1.5 times the thermal parameter of the carbon atom to which it was attached. For the methyl groups, where the location of the hydrogen atoms is uncertain, the AFIX 137 card was used to allow the hydrogen atoms to rotate to the maximum area of residual density, while fixing their geometry. In cases of extreme disorder, the non-hydrogen atoms were refined only isotropically, and hydrogen atoms were not included in the model (see Supporting Information). Structural and refinement data for all of the complexes are presented in Tables 1, 4, and 7. Individual aspects of the structures are given in the Supporting Information. ORTEP diagrams were drawn using the ORTEP-3 for Windows package,²⁴ while the space-filling representations were rendered using MolPOV 2 for Windows.²⁵

Results and Discussion

Lithium Salts. The reaction of *n*-butyllithium with tris(3,5-di-*tert*-butyl-2-hydroxyphenyl)methane **1a** dissolved in benzene, if left undisturbed, readily yields colorless crystals of the lithium salt, **2a**. The compound was fully characterized by NMR and elemental analysis. Proton NMR clearly demonstrates that the 3-fold symmetry of the starting material has been retained. Additionally, the absolute conformation and geometry of **2a** was established by a single-crystal X-ray crystallographic study.

(24) Farrugia, L. J. *J. Appl. Crystallogr.* **1997**, 565.

(25) Richardson, D. E., Department of Chemistry, University of Florida.

(23) Blessing, R. H. *Acta Crystallogr.* **1995**, A51, 33.

Table 1. X-ray Data^a for the Crystal Structures of the Complexes **2a**, **3a**·6THF·²/₃THF, **3b**·6CH₂Cl₂·2.6CH₂Cl₂, **4a**·6THF·THF, and **4c**·6THF·¹/₄THF

	2a	3a ·6THF· ² / ₃ THF	3b ·6CH ₂ Cl ₂ ·2.6CH ₂ Cl ₂	4a ·6THF·THF	4c ·6THF· ¹ / ₄ THF
total reflns	28815	39160	16493	39516	56299
unique reflns	10498	14389	3568	14735	10012
collection range	1.79° < θ < 29.39°	1.65° < θ < 29.40°	1.68° < θ < 25.00°	1.75° < θ < 29.36°	1.71° < θ < 26.38°
T _{max,min}	1.00, 0.61	1.00, 0.87	1.00, 0.63	1.00, 0.88	1.00, 0.60
empirical formula	C ₈₆ H ₁₂₂ O ₆ Li ₆	C _{112.67} H _{175.34} O _{12.67} Na ₆	C _{106.6} H _{163.2} O ₆ Na ₆ Cl _{17.2}	C ₁₁₄ H ₁₇₈ O ₁₃ K ₆	C ₉₃ H ₁₃₆ O _{12.25} K ₆
M _r	1293.48	1870.42	2288.45	1991.16	1684.92
cryst syst	monoclinic	monoclinic	hexagonal	monoclinic	orthorhombic
space group	P2 ₁ /c	P2 ₁ /n	R3	P2 ₁ /n	Pccn
a (Å)	13.8313(9)	14.3125(2)	14.423(2)	14.436(1)	18.5828(5)
b (Å)	23.326(2)	18.2525(4)		18.3559(1)	18.6385(6)
c (Å)	14.3529(9)	21.9963(4)	50.468(8)	22.1571(2)	28.3267(9)
α (deg)					
β (deg)	115.191(1)	93.497(1)		94.538(1)	
γ (deg)					
V _c (Å ³)	4190.2(5)	5735.6(2)	9092(2)	5852.95(6)	9811.1(5)
D _c (g cm ⁻³)	1.025	1.083	1.254	1.130	1.140
Z	2	2	3	2	4
F(000)	1408	2037	3628	2160	3624
μ(Mo Kα) (mm ⁻¹)	0.061	0.088	0.458	0.278	0.320
R1 [I ≥ 2σ(I) data] ^b	0.0608 [7333]	0.0731 [9413]	0.0681 [3138]	0.0683 [9149]	0.0733 [6023]
wR2 (all data); X, Y ^c	0.1568; 0.0578, 1.67	0.2350; 0.1117, 5.05	0.1928; 0.0988, 24.20	0.2105; 0.1036, 3.17	0.2362; 0.1268, 10.56
GOF	1.021	1.052	1.098	1.053	1.008
largest peak, deepest trough (e Å ⁻³)	+0.22, -0.26	+0.86, -0.34	+0.75, -0.63	+0.96, -0.50	+0.94, -0.51

^a Obtained with monochromatic Mo Kα radiation (λ = 0.71073 Å). ^b R1 = Σ||F_o| - |F_c||/Σ|F_o|. ^c wR2 = {Σ[w(F_o² - F_c²)/Σ[w(F_o²)]}^{1/2} where w = 1/[σ²(F_o²) + (XP)² + YP] where P = (F_o² + 2F_c²)/3.

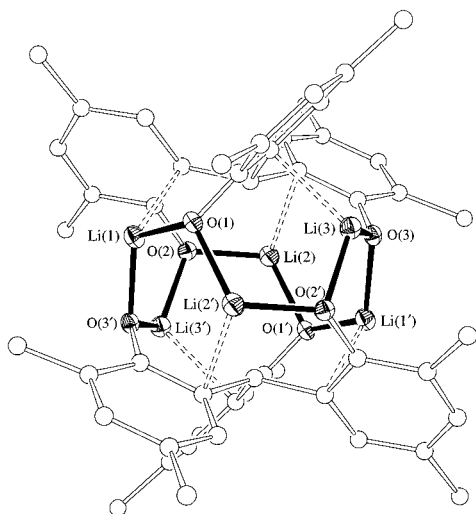


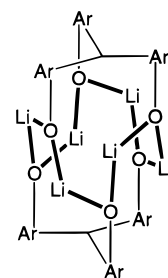
Figure 2. ORTEP (30% ellipsoids) representation of **2a**, with carbon atoms depicted as spheres. For clarity, the core has been drawn with solid lines, and the hydrogen atoms and *tert*-butyl methyl groups have been omitted. The numbering scheme follows that depicted in Figure 1, with the remainder of the structure, denoted by primed and unprimed atoms, related by a center of inversion.

Figure 1 describes the atom-numbering scheme, while Figure 2 depicts the hexanuclear aggregate **2a**. Collection parameters are shown in Table 1, while selected bond lengths and angles are presented in Table 2.

The structure, overall, bears a remarkable resemblance to that of the starting material **1a**, which, in the solid state, is a hydrogen-bonded dimer,²¹ and in **2a** the lithium atoms essentially reside in the hydrogen atom positions in **1a**. Each lithium bonds to only two oxygen atoms, since they have insufficient size to bridge an adjacent oxygen atom (at 3.24 Å) and the aggregate is too sterically crowded for solvent molecule coordination. Instead, there may exist a weak interaction with the *tert*-butyl methyl groups, since these carbon atoms are only

2.594(3), 2.608(3), and 2.638(3) Å distant from Li(1), Li(2), and Li(3), respectively.

More important interactions are evident between the aromatic carbons and lithium atoms: significant ones for the lithiums and C(2), C(16), and C(30) (those bound to the central carbon) with an average distance of 2.310(3) Å, and possibly a weak one with the *ipso*-phenolate carbons at an average distance of 2.603(5) Å. The aromatic rings in the aggregate are also canted appreciably relative to the aggregate core, but these interactions only marginally affect the geometry of the ligand in comparison with the starting material **1a**. From a least-squares plane drawn through O(1)–O(2)–O(3) in **1a**, the angles between the three rings are 45.8°, 48.3°, and 41.4°, respectively, while the analogous angles are 42.2°, 41.0°, and 40.3° in **2a**.



2a Ar = 3,5-di-*tert*-butyl-phenyl

Although the lithium salt **2a** shows low solubility in common organic solvents save THF, a weak ¹H NMR spectrum of **2a** in C₆D₆ could be obtained (Figure 3). Besides the absence of the OH proton resonance, the spectrum is not markedly different from that of the free tris-phenol **1a** (Figure 3). The most significant and diagnostic signal, the central methine proton, exhibits a moderate downfield shift, from 5.90 in **1a** to 6.38 ppm in **2a**, possibly resulting from only a minor structural change in the formation of **2a** together with a significant electronic one, although the sodium and potassium salts feature much larger downfield shifts, *vide infra*. Unfortunately, the very

Table 2. Selected Bond Lengths (Å) and Angles (deg) for the Compounds **2a**, **3a**·6THF·²/₃THF, **3b**·6CH₂Cl₂·2.6CH₂Cl₂, and **3a**·2Et₂O·2²/₃Et₂O^a

2a		3a ·6THF· ² / ₃ THF		3b ·6CH ₂ Cl ₂ ·2.6CH ₂ Cl ₂ [equivalent atoms]		3a ·2Et ₂ O·2 ² / ₃ Et ₂ O
		Na(1)···O(101)	2.383(2)	2.891(1)		2.447(5)
		Na(2)···O(201)	2.412(2)			
		Na(3)···O(301)	2.396(2)			
Li(1)–O(1)	1.828(3)	Na(1)–O(1)	2.298(2)	2.280(2)		2.299(4)
Li(1)–O(3)	3.241(3)	Na(1)–O(2)	2.348(2)	2.326(2)	[O(1 ^{II})]	2.451(4)
Li(1)–O(3')	1.874(3)	Na(1)–O(3')	2.280(2)	2.246(2)	[O(1 ^I)]	2.333(4)
Li(1)···C(17)	2.609(3)	Na(1)···C(17)	2.764(2)	2.771(3)	[C(3 ^{III})]	2.691(6)
Li(2)···C(31)	2.623(3)	Na(2)···C(31)	2.812(2)			2.681(5)
Li(3)···C(3)	2.577(3)	Na(3)···C(3)	2.791(2)			2.668(6)
Li(1)···C(16)	2.309(3)	Na(1)–C(16)	3.102(2)			
Li(2)···C(30)	2.303(3)	Na(2)–C(30)	3.100(2)			
Li(3)···C(2)	2.317(3)	Na(3)–C(2)	3.045(2)			
Σ[C _{ipso} –C(1)–C _{ipso}]	341.0(2)	Σ[C _{ipso} –C(1)–C _{ipso}]	338.1(3)	338.1(3)		336.6(7)
Li(1)–O(1)–Li(2')	108.3(1)	Na(1)–O(1)–Na(3)	126.00(8)	125.03(8)	[Na(1 ^{IV})]	127.9(2)
		Na(1)–O(1)–Na(2')	87.35(7)	86.36(6)	[Na(III)]	88.4(1)
		O(1)–Na(1)–O(2)	110.19(7)	112.90(9)	[O(1 ^{II})]	109.2(1)
		O(1)–Na(1)–O(3')	93.97(7)	93.21(7)	[O(1 ^I)]	93.0(1)
		O(2)–Na(1)–O(3')	91.41(7)	94.47(7)	[O(1 ^{II})/O(1 ^I)]	88.1(1)
		O(1)–Na(1)–O(101)	105.97(9)	103.91(6)		102.5(2)
		O(2)–Na(1)–O(101)	118.25(8)	118.92(6)	[O(1 ^{II})]	122.8(2)
		O(3')–Na(1)–O(101)	133.91(8)	131.18(6)	[O(1 ^I)]	136.7(2)

^a Corresponding lengths and angles are given in the same rows.

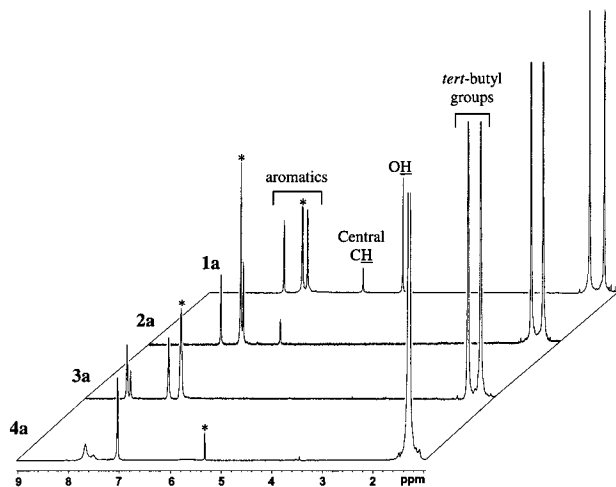


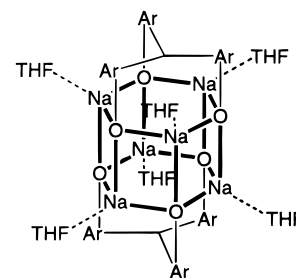
Figure 3. ¹H NMR (300 MHz) spectra of **1a**, **2a** (lithium), and **3a** (sodium) in C₆D₆ solvent, and **4a** (potassium) in CD₂Cl₂. Residual C₆D₆ and CH₂Cl₂ are denoted by asterisks (*).

poor solubility of **2a** precluded acquisition of a ¹³C spectra in common unreactive deuterated solvents. Compound **2a** is, however, easily soluble in tetrahydrofuran, so a ¹³C NMR was recorded in *d*₈-THF. Although care should be taken when comparing data for this spectrum with spectral data for the other compounds, it is clear that the carbon spectrum is fairly similar to the CDCl₃ spectra of **1a**. Indeed, the central carbon resonance appearing at 42.5 ppm is in the same position as that in **1a** (CDCl₃). The most significant difference witnessed in the ¹³C NMR spectra of the two compounds is the phenoxide *ipso*-carbon, which in **2a** appears at 163.8 ppm, compared to 150.8 ppm in **1a**.

Since the lithium salt features no accessible coordination sites, its utility for chemistry is probably very limited, and studies of this system were not pursued further.

Sodium Salts. The reaction of **1a** with an excess of sodium hydride in tetrahydrofuran at room temperature for 18 h produces, after filtration, the hexanuclear aggregate **3a**·6THF as the sole product. The material was characterized by NMR, high-resolution FAB mass spectrometry, and a single-crystal

X-ray structure, although satisfactory microanalytical data could not be obtained for this compound, due to the relative volatility of the THF molecules; indeed, they can be completely removed with evacuation and gentle warming. The analogous, albeit slightly more sterically demanding system **3b** could be similarly formed from **1b** and sodium hydride, although refluxing conditions were required in this case.



3a Ar = 3,5-di-*tert*-butyl-phenyl

3b Ar = 3,5-di-*tert*-pentyl-phenyl

Figure 4 shows the structure of **3a**·6THF·²/₃THF, the atom-numbering scheme follows that in Figure 1, and structural parameters are shown in Table 1, with selected bond lengths and angles presented in Table 2.

The sodium salt **3a**·6THF features many structural similarities with the lithium salt **2a**. Both are hexanuclear aggregates, with two triarylmethane units above and below the metal cluster. In this system, however, the larger radius of the sodium cation allows it to bridge a third aryloxy oxygen to give a core essentially composed of two stacked Na₃O₃ hexagons. These hexagons are fairly close to planar, with an average deviation of 0.87 Å above and below (relative to the ligand) the least-squares plane, for the sodium and oxygens, respectively. Surprisingly, this Na₆O₆ core has been structurally characterized only once previously,²⁶ although M₆O₆ cores of this type have been seen previously for aluminum²⁷ and titanium,²⁸ with numerous examples for tin²⁹ and, more relevantly, for lithium.³⁰

(26) Schutte, S.; Klingebiel, U.; Schmidt-Base, D. *Z. Naturforsch., Teil B* **1993**, *48*, 263.

(27) Mason, M. R.; Smith, J. M.; Bott, S. G.; Barron, A. R. *J. Am. Chem. Soc.* **1993**, *115*, 4971.

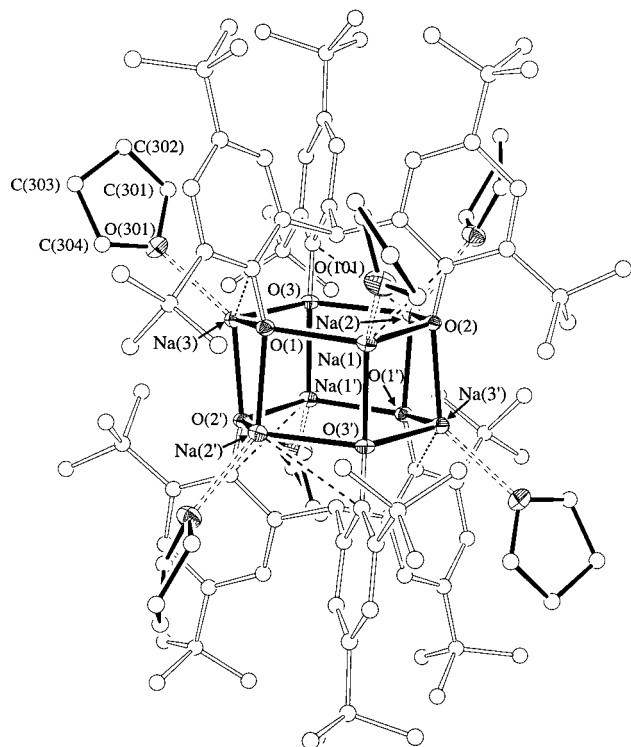


Figure 4. ORTEP (30% ellipsoids) representation of $3\mathbf{a}\cdot 6\text{THF}\cdot 2/3\text{THF}$, with carbon atoms depicted as spheres. For clarity, the THF molecules and the aggregate core have been drawn with solid lines. The numbering scheme follows that depicted in Figure 1. The additional lattice THF solvate has been omitted, together with the hydrogen atoms. Only one of the THF molecules has been numbered completely, with the remaining two unique THF molecules [O(201)–C(204) and O(301)–C(304)] numbered analogously. The remainder of the structure, denoted by primed and unprimed atoms, is related by an inversion center.

The sodium phenoxide bond lengths are typical, 2.298(2)–2.349(2) Å, which compares with distances of 2.231(3)–2.403(2) Å in the structure of the related phenoxide salt hexakis(phenoxo-tetrahydrofuran-sodium).³¹ For the only other structure with a core analogous to $3\mathbf{a}$ (derived from di-*tert*-butylsilandiol),²⁶ bond lengths corresponding to Na(1)–O(1), Na(2)–O(2), and Na(1)–O(3') in $3\mathbf{a}$ of 2.239(3), 2.412(3), and 2.273(3) Å, respectively, were measured. These follow the same trend observed in the structures of $3\mathbf{a}$, in that alternating long and short bonds are seen in the two hexagons, with the distance between the two hexagons being short. The cause for the alternating bond lengths can be attributed to the sodium *ipso*-carbon interactions, which are on average 2.79(2) Å, and these contacts effectively weaken the associated Na–O bonds. The more pronounced bond differences seen in the silanediol salt

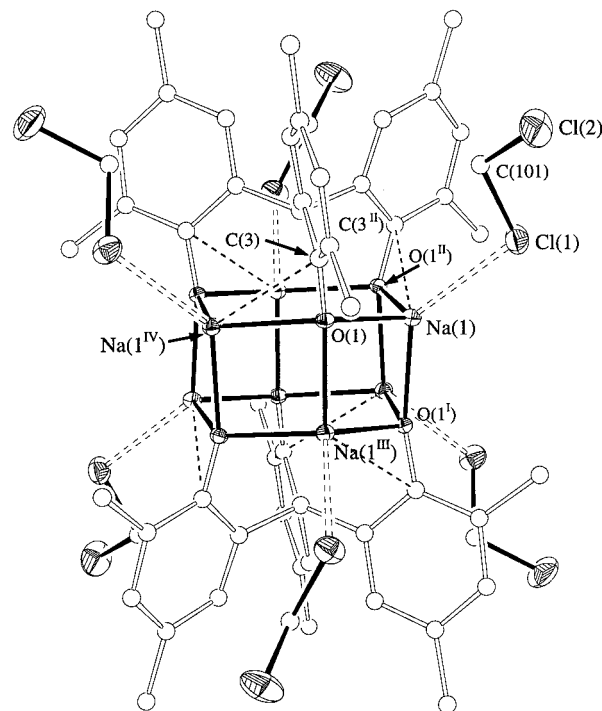
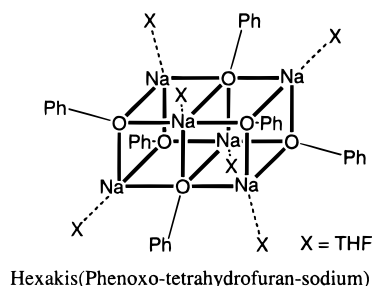


Figure 5. ORTEP representation of $3\mathbf{b}\cdot 8.6\text{CH}_2\text{Cl}_2$ (30% probability ellipsoids), with carbon atoms depicted as spheres. The cluster resides on an S_6 symmetry position, relating all of the sodium atoms, aromatic rings, and dichloromethanes. Only the tertiary amyl carbon is shown, and hydrogen atoms and dichloromethane solvate molecules have also been omitted for clarity.

are similarly attributed to coordination, although in this case it is from a free hydroxide donating to a neighboring sodium.²⁶ In accord with this observation, the aromatic rings in $3\mathbf{a}\cdot 6\text{THF}$ are clearly not orientated perpendicular to the Na_6O_6 core, rather, they are canted by 80.6–82.2°, presumably so that the adjacent sodium can maximize its interaction with phenolate *ipso*-carbon.



In the Na_6O_6 aggregate, each of the six sodium cations adopts a distorted tetrahedral arrangement. The extent of the distortion is readily witnessed in the angles around the sodiums; angles of 93.97(7)° and 91.41(7)° are noted for O(1)–Na(1)–O(3') and O(2)–Na(1)–O(3'), respectively. The remaining coordination site on each sodium is occupied by a THF molecule at an average distance of 2.397(4) Å. This bond is marginally longer than that measured in the related sodium phenoxide system, which features Na–THF bond lengths of ~2.31 Å.³¹

In an attempt to isolate a sodium aggregate free of coordinated solvent, we recrystallized $3\mathbf{b}$ from the poorly donating dichloromethane by diffusion of pentane into a dichloromethane solution of $3\mathbf{b}$. Figure 5 depicts the structure of the complex, with selected bond lengths and angles shown in Table 2.

Aside from the differences of the ring alkyl substituents and coordinating solvent, the general conformation of this species

- (28) Carofiglio, T.; Floriani, C.; Roth, A.; Sgamellotti, A.; Rosi, M.; Chiesi-Villa, A.; Rizzoli, C. *J. Organomet. Chem.* **1995**, *488*, 141.
- (29) See, for example: Alcock, N. W.; Roe, S. M. *J. Chem. Soc., Dalton Trans.* **1989**, 1589.
- (30) (a) Jastrzebski, J. T. B. H.; van Koten, G.; van de Mierop, W. F. *Inorg. Chim. Acta* **1988**, *142*, 169. (b) Chisholm, M. H.; Drake, S. R.; Nairni, A. A.; Streib, W. E. *Polyhedron* **1991**, *10*, 805. (c) Jones, R. A.; Koschmieder, S. U.; Atwood, J. L.; Bott, S. G. *J. Chem. Soc., Chem. Commun.* **1992**, 726. (d) Herberich, G. E.; Spaniol, T. P.; Fischer, A. *Chem. Ber.* **1994**, *127*, 1619. (e) Goldfuss, B.; von Ragué Schleyer, P.; Hampel, F. *Organometallics* **1997**, *16*, 5032. (f) Brask, J. K.; Chivers, T.; Parvez, M.; Schatte, G. *Angew. Chem., Int. Ed. Engl.* **1997**, *36*, 1986. (g) Goldfuss, B.; von Ragué Schleyer, P. v. R.; Hampel, F. *J. Am. Chem. Soc.* **1996**, *118*, 12183. (h) Jackman, L. M.; Cizmeciyan, D.; Williard, P. G.; Nichols, M. A. *J. Am. Chem. Soc.* **1993**, *115*, 6262.
- (31) Kunert, M.; Dinjus, E.; Nauck, M.; Sieler, J. *Chem. Ber.-Recl.* **1997**, *130*, 1461.

is analogous to the THF adduct, **3a**·6THF, discussed above. The phenoxide oxygen coordination spheres of the sodiums are also comparable, although the bond lengths are significantly shorter (0.018–0.034 Å) in the dichloromethane adduct, as would be expected for sodiums with appreciably less electron density. An additional useful measurement is how far the sodium cations reside above the plane defined by the three respective bonding phenoxide oxygens. This gives the degree of pyramidal for the sodiums. As expected for a weaker donor atom, the sodiums are 1.05 Å above the plane for **3b**·6CH₂Cl₂, compared with 1.10 Å for **3a**·6THF. This contraction produces a tighter/more compact structure, although the Na–*ipso*-carbon interactions [average 2.789(4) Å for **3a**·6THF and 2.771(3) Å for **3b**·6CH₂Cl₂], are comparable.

A weak interaction [Na···Cl(1) 2.891 Å] is evident between the sodium and dichloromethane solvent chlorine atom. Surprisingly, a search of the Cambridge Crystallographic Database reveals that structurally characterized interactions of this type are in fact extremely rare, and to the best of our knowledge they have been reported for sodium only once previously.³² In addition to this example, several late transition metal complexes (Pt,³³ Ru,³⁴ and Ag³⁵) with coordinating dichloromethane molecules have been published. For the lone example involving sodium, which was also derived from an aryloxide, the Na···Cl distance was found to be 2.858(2) Å, marginally shorter than in **3b**·6CH₂Cl₂. Further evidence for the Na···Cl interaction is seen in the slight, but perceptible, difference in Cl–C bond lengths of the coordinated [1.774(3) Å] and noncoordinated [1.747(3) Å] chlorine atoms. The lengthening of the coordinated Cl–C bond distance can be interpreted as a decrease of electron density in this atom. A comparable lengthening of the sodium–chlorine bond of 0.042(3) Å was also seen for the related sodium phenoxide system.³² The presence of these weakly bound dichloromethane molecules further demonstrates the electrophilic nature of the sodium cations in **3**.

The ¹H and ¹³C NMR spectra of the Na₆O₆ compounds, **3**, are entirely consistent with the X-ray structures. In comparison to both **1a** and **2a**, the central methine proton is shifted downfield in the ¹H NMR spectrum (Figure 3) of solvent-free **3a**, to 8.15 ppm. This shift possibly reflects the significant geometry difference, and the subsequent electronic effects, relative to the starting material or **2a**, since the electronegativities of sodium and lithium are comparable.³⁶ Similarly, in the ¹³C NMR spectrum of **3a**, the central carbon appears at 31.6 ppm, 10.9 ppm upfield from the starting material **1a**. The only other diagnostic signal is the phenoxide *ipso*-carbon, which, as expected, is significantly upfield in **3a** at 161.7 ppm, relative to 150.8 ppm in **1a**.

Potassium Salts. Tris(3,5-di-*tert*-butyl-2-hydroxyphenyl)methane **1a** was dissolved in THF and reacted with potassium hydride in a fashion analogous to that used in the synthesis of the sodium salts. After workup, a white, extremely moisture sensitive powder was collected. The material has negligible solubility in most common organic solvents, although a ¹H NMR spectrum was collected in *d*₂-dichloromethane. Crystallization by evaporation of a THF solution yielded colorless blocks suitable for X-ray crystallographic analysis. Figure 6 depicts

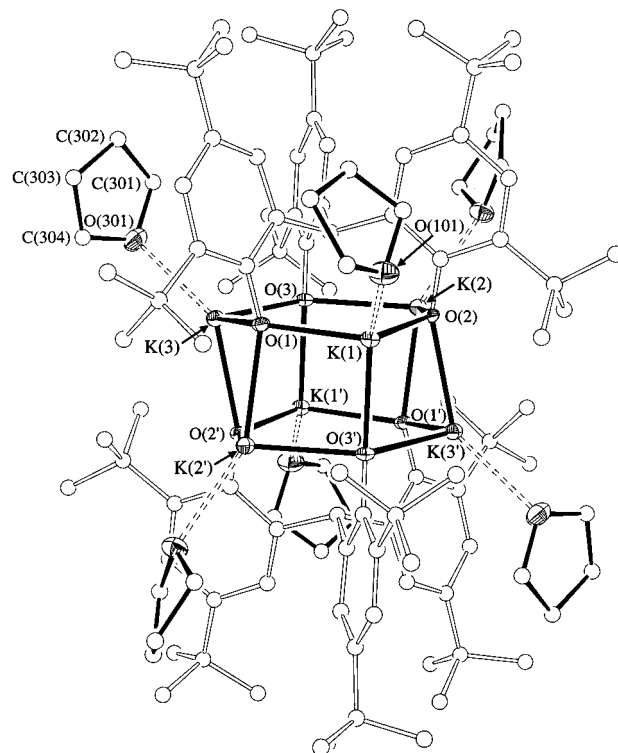


Figure 6. ORTEP (30% ellipsoids) representation of **4a**·6THF·THF, with carbon atoms depicted as spheres. For clarity, the THF molecules and the aggregate core have been drawn with solid lines. The numbering scheme follows that depicted in Figure 1. The additional lattice THF solvate has been omitted, together with the hydrogen atoms. Only one of the THF molecules has been numbered completely, and the remaining two unique THF molecules are numbered analogously. The remainder of the structure, denoted by primed and unprimed atoms, is related by an inversion center.

Table 3. Selected Bond Lengths (Å) and Angles (deg) for the Compounds **4a**·6THF·THF and **4c**·6THF·¹/₄THF

	4a ·6THF·THF	4c ·6THF· ¹ / ₄ THF [equivalent atoms]	
K(1)···O(1014)	2.753(3)	2.689(4)	
K(2)···O(201)	2.716(2)	2.672(4)	
K(3)···O(301)	2.688(3)	2.718(4)	
K(1)–O(1)	2.570(2)	2.569(3)	
K(1)–O(2)	2.635(2)	2.732(3)	
K(1)–O(3')	2.647(2)	2.649(3)	
K(1)···C(17)	2.946(3)	2.899(4)	[C(13)]
K(2)···C(31)	2.979(3)	2.887(4)	[C(24)]
K(3)···C(3)	2.945(3)	2.909(4)	
Σ[C _{ipso} –C(1)–C _{ipso}]	337.3(3)	335.5(5)	
O(1)–K(1)–O(2)	98.55(6)	103.93(9)	
O(1)–K(1)–O(3')	88.03(6)	90.75(9)	
O(2)–K(1)–O(3')	86.12(6)	93.13(8)	
K(1)–O(1)–K(3)	136.45(8)	133.2(1)	
K(1)–O(1)–K(2')	89.99(6)	84.31(8)	
O(1)–K(1)–O(101)	110.23(8)	117.6(1)	
O(2)–K(1)–O(101)	124.62(7)	124.3(1)	
O(3')–K(1)–O(101)	138.97(8)	120.1(1)	

the structure, and Tables 1 and 3 present the crystallographic data and selected bond lengths and angles, respectively, while the numbering scheme follows that shown in Figure 1.

The structure bears a very strong resemblance to that observed for the sodium-based structures outlined above, except for an important distinction. The larger ionic radius of potassium forces an increase in the metal–oxygen distance of approximately 0.32 Å relative to **3a**·6THF, and the tris(3,5-dialkyl-2-phenoxy)methane ligand cannot accommodate these larger cations as well

(32) Gordon, B. W. F.; Scott, M. J. *Inorg. Chim. Acta* **2000**, 297, 206.

(33) Butts, M. D.; Scott, B. L.; Kubas, G. J. *J. Am. Chem. Soc.* **1996**, 118, 11831.

(34) Bown, M.; Waters, J. M. *J. Am. Chem. Soc.* **1990**, 112, 2442.

(35) Colman, M. R.; Newbound, T. D.; Marshall, L. J.; Noirot, M. D.; Miller, M. M.; Wulfsberg, G. P.; Frye, J. S.; Anderson, O. P.; Strauss, S. H. *J. Am. Chem. Soc.* **1990**, 112, 2349 and references therein.

(36) Allred, A. L. *J. Inorg. Nucl. Chem.* **1961**, 17, 215.

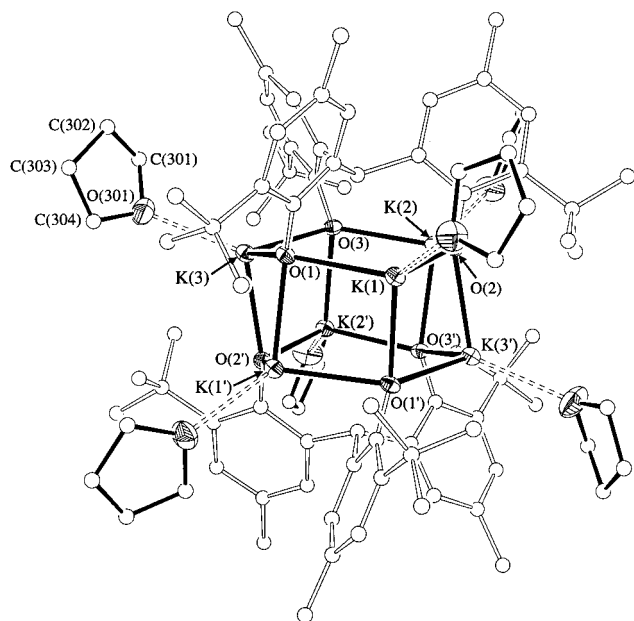


Figure 7. ORTEP (30% ellipsoids) representation of $4\mathbf{a}\cdot 6\text{THF}\cdot \frac{1}{4}\text{THF}$, with carbon atoms depicted as spheres. For clarity, the THF molecules and the aggregate core have been drawn with solid lines. The numbering scheme follows that depicted in Figure 1. The THF solvate has been omitted, together with the hydrogen atoms. Only one of the THF molecules has been numbered completely, and the remaining two unique THF molecules are numbered analogously. The remainder of the structure, denoted by primed and unprimed atoms, is related by an inversion center.

as sodium. As a result, each potassium center must adopt a structure with an even greater degree of deformation away from tetrahedral in comparison with $3\mathbf{a}$ and $3\mathbf{b}$, with the potassium atoms puckered out of the hexagonal core. The potassiums average 1.45 Å above the plane defined by bonding phenoxide oxygens, compared with 1.10 Å measured for the sodium atoms in $3\mathbf{a}\cdot 6\text{THF}$. The O–K–O core angles range from 86° to 99° on average, considerably more acute than the corresponding angles in the sodium system, which range from 91° to 110°. Much like in $3\mathbf{a}\cdot 6\text{THF}$, the rings in $4\mathbf{a}\cdot 6\text{THF}$ are canted relative to the K_6O_6 core, and to a similar degree [80.6–82.3°]. The potassiums thus make an average approach to the phenolic *ipso*-carbons of 2.957(5) Å. The remaining structural details are analogous to those of $3\mathbf{a}$.

Comparing the geometry around the central carbon linker [C(1)] by examination of the sum of the $\text{C}_{\text{ipso}}\text{--C}(1)\text{--C}_{\text{ipso}}$ angles of $4\mathbf{a}\cdot 6\text{THF}$ with the free ligand $1\mathbf{a}$ [$\text{S}\{\text{C}_{\text{ipso}}\text{--C}(1)\text{--C}_{\text{ipso}}\}$ 338.9–(3)°], the lithium salt $2\mathbf{a}$, and the sodium salt $3\mathbf{a}$, it is clear no significant changes are measured, highlighting the relative rigidity of the platform.

In order to assess the effect of changes in the steric properties of the tris(3,5-dialkyl-2-phenoxy)methane ligand on the conformation of the aggregate, the potassium salt of the less sterically crowded tris(3-*tert*-butyl-5-methyl-2-hydroxyphenyl)methane $1\mathbf{c}$ was prepared and crystallized. As revealed by the single-crystal X-ray structure of this compound $4\mathbf{c}\cdot 6\text{THF}$ (Figure 7), the potassium maintains a tetrahedral orientation, with bond lengths comparable to those of $4\mathbf{a}$. Although the metal is still strained, the O–K–O bond angles are able to relax closer to tetrahedral (90.64–101.46°), relative to $4\mathbf{a}\cdot 6\text{THF}$. With the less sterically encumbering groups, the phenoxide arms have increased flexibility, and the ligand can better accommodate the binding desires of the metals. Consequently, the aromatic rings exhibit a much greater degree of canting relative to the cluster

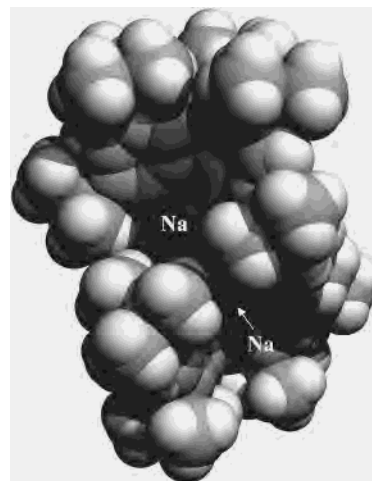


Figure 8. Space-filling representation of the crystal structure of $3\mathbf{a}\cdot \text{THF}\cdot \frac{2}{3}\text{THF}$, with all THFs deleted to reveal the binding “pockets”.

core. Of the six rings in $4\mathbf{c}\cdot 6\text{THF}$, two adopt a position 66.8° from the aggregate core while the other four are bent by 73.3°, an average of 10.2° less than that seen in $4\mathbf{a}$, in which the *tert*-butyl groups force the six rings into an orientation much closer to perpendicular to the core. Additionally, the *ipso*-carbon interactions with the potassiums are also statistically shorter, showing an average distance of 2.898(6) Å [cf. 2.957(5) Å seen in $4\mathbf{a}$], concomitant with a ~0.1 Å lengthening of the K(1)–O(2) distance, for reasons discussed previously for $3\mathbf{a}\cdot 6\text{THF}$.

Due to the extremely low solubility of $4\mathbf{a}$ and $4\mathbf{b}$ in organic solvents, including THF, NMR analysis proved difficult, but a weak ^1H spectrum of solvent-free $4\mathbf{a}$ could be obtained in CD_2Cl_2 (Figure 3). The peaks were found to be very broad, indicating that a fluxional process occurs on the NMR time scale. Unfortunately, the insolubility of the material precluded acquisition of a low-temperature ^1H NMR, and the low boiling point of dichloromethane hinders determination of high-temperature spectra. Besides the broadness of the signals, the room temperature NMR of $4\mathbf{a}$ shows peak positions comparable to those of $3\mathbf{a}$, which would be expected, given their structural similarity. When the ^1H NMR of $3\mathbf{a}$ was acquired in CD_2Cl_2 , the central methine proton resonated at 7.91 ppm, with this proton appearing as a broad signal at 7.55 ppm in the spectrum of $4\mathbf{a}$.

Sodium Salt Adducts. From a careful examination of the structures of $3\mathbf{a}\cdot 6\text{THF}$ and $3\mathbf{b}\cdot 6\text{CH}_2\text{Cl}_2$, it is evident that the solvent molecules reside in well-defined “pockets” created by the aromatic rings and their substituents in the 3- and 5-positions. Figure 8 shows a space-filling representation of the structure of $3\mathbf{a}\cdot 6\text{THF}$ with the THF molecules omitted. With a confined space around the metal, these electrophilic sodiums should be accessible only to molecules that possess a size and shape compatible with these “pockets”, and we undertook an examination of the binding properties of $3\mathbf{a}$. A number of oxygen donor molecules were explored, with particular emphasis on ketones and aldehydes, since these compounds are useful precursors for the synthetic chemist. The results of these studies follow.

Ethers. As already witnessed, the sodium salts readily accommodate both THF and dichloromethane; thus, larger ether molecules were explored. Early on, it was apparent in the studies that diethyl ether either does not bind or binds only very weakly, since the majority of the compounds subsequently described can be synthesized directly in diethyl ether solvent. Attempts to crystallize $3\mathbf{a}$ out of ether proved quite difficult, due to the tendency of crystals to form as feathery plates, but crystals

Table 4. X-ray Data^a for the Crystal Structures of the Diethyl Ether and Aldehyde Adducts of **3a**

	3a ·2Et ₂ O·2 ² / ₃ Et ₂ O	3a ·6C ₇ H ₆ O·2C ₆ H ₆ ·0.8C ₅ H ₁₂ (benzaldehyde)	3a ·6C ₉ H ₈ O· ¹ / ₂ Et ₂ O (<i>trans</i> -cinnamaldehyde)	3a ·6C ₁₀ H ₁₄ O·Et ₂ O (safranal)
total reflections	22181	20205	43729	43510
unique reflections	6951	13516	29527	14975
collection range	1.63° < θ < 22.50°	1.58° < θ < 26.38°	1.30° < θ < 27.50°	1.37° < θ < 26.39°
$T_{\max, \min}$	1.00, 0.88	1.00, 0.74	1.00, 0.85	1.00, 0.88
empirical formula	C _{104.67} H _{168.67} O _{10.67} Na ₆	C ₁₄₄ H _{179.6} O ₁₂ Na ₆	C ₁₄₂ H ₁₇₅ O _{12.5} Na ₆	C ₁₅₀ H ₂₁₆ O ₁₃ Na ₆
M_r	1735.66	2238.80	2219.76	2365.17
cryst syst	monoclinic	triclinic	triclinic	monoclinic
space group	$P2_1/n$	$P1$	$P2_1/n$	$P2_1/n$
a (Å)	14.0195(6)	14.2323(2)	17.5872(3)	18.3501(8)
b (Å)	26.782(1)	14.8545(3)	18.4231(3)	20.4710(9)
c (Å)	14.3197(7)	18.3521(4)	24.0992(3)	19.9503(9)
α (deg)		105.439(1)	75.143(1)	
β (deg)	98.025(1)	109.517(1)	89.762(1)	102.172(1)
γ (deg)		99.182(1)	64.039(1)	
V_c (Å ³)	5323.9(4)	3390.6(1)	6733.1(2)	7325.7(6)
D_c (g cm ⁻³)	1.083	1.096	1.095	1.072
Z	2	1	2	2
$F(000)$	1896	1204	2386	2572
μ (Mo K α) (mm ⁻¹)	0.088	0.084	0.084	0.081
R1 [$I \geq 2\sigma(I)$ data] ^b	0.0828 [4293]	0.0833 [7495]	0.0755 [19038]	0.0727 [6376]
wR2 (all data); X, Y^c	0.2622; 0.1432, 9.47	0.2719; 0.1412, 1.53	0.2221; 0.0834, 6.21	0.2582; 0.1250, 0.00
GOF	1.017	1.033	1.100	0.987
largest peak, deepest trough (e Å ⁻³)	+1.18, -0.53	+0.87, -0.74	+1.31, -0.27	+0.91, -0.56

^a Obtained with monochromatic Mo K α radiation ($\lambda = 0.71073$ Å). ^b $R1 = \sum ||F_o| - |F_c|| / \sum |F_o|$. ^c $wR2 = \{ \sum [w(F_o^2 - F_c^2)^2 / \sum [w(F_o^2)^2]] \}^{1/2}$ where $w = 1 / [\sigma^2(F_o^2) + (XP)^2 + YP]$ where $P = (F_o^2 + 2F_c^2) / 3$.

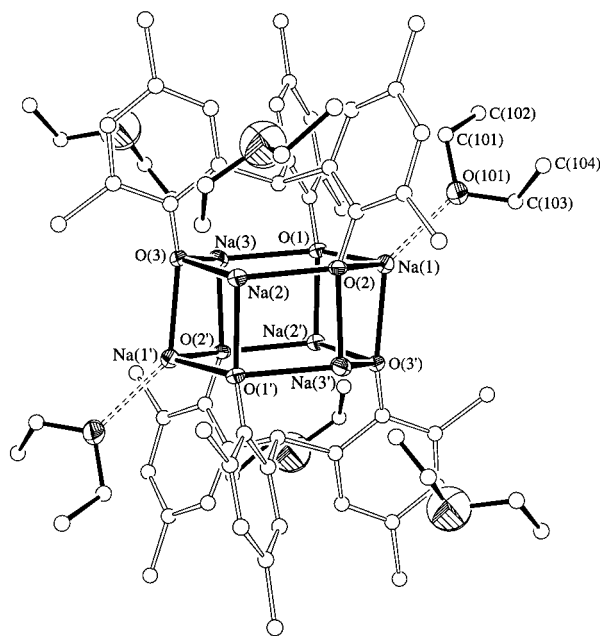


Figure 9. ORTEP (30% ellipsoids) representation of **3a**·2Et₂O·2²/₃Et₂O, with carbon atoms depicted as spheres. For clarity, the ether molecules and the aggregate core have been drawn with solid lines. The numbering scheme follows that depicted in Figure 1. The additional lattice *tert*-butyl methyl groups and hydrogen atoms have been omitted. Only one of the ether molecules has been numbered with the remaining two uncoordinated ether molecules numbered analogously. The remainder of the structure, denoted by primed and unprimed atoms, is related by an inversion center.

suitable for X-ray characterization were eventually obtained after many attempts. Figure 9 depicts the structure, data collection parameters can be found in Table 4, and selected bond lengths and angles are presented in Table 2.

Unfortunately, the crystals contained highly disordered ether solvates. The atoms refined poorly, with large thermal parameters and residual density persisting in electron density maps. For this reason, the structure is not discussed in detail, and the

bond length and angle values, with the exception of the core, should be treated with some caution. Nevertheless, the overall conformation and connectivity is unambiguous, and it is clear that two ethers are coordinated to sodium atoms, while four, unbound, disordered solvents reside end-on in the pockets. We interpret this data with the notion that in order for the aggregate to accommodate even two ethers, a slight structural rearrangement must take place, effectively blocking the remaining four vacant sodium sites for coordination. Unsurprisingly, the pyramidality for the sodiums with coordinated solvent compared with those without is markedly different. The sodium Na(1), which has ether bound, is 1.17 Å above its phenoxide plane, whereas the remaining two uncoordinated sodiums, Na(2) and Na(3), are only 1.02 and 0.99 Å above their respective planes. In solution, the binding of the ethers is probably a reversible, fluxional process, since ¹H NMR spectra still exhibit C_3 -symmetry for the ligand. On the basis of these findings, ether was chosen as the solvent for the binding studies.

While THF readily binds to the sodium aggregate **3a**, ¹H NMR studies suggest that the addition of an excess of a mixture of *cis*- and *trans*-2,5-dimethyltetrahydrofuran to a solution of **3a** in deuterated benzene results in no coordination of the substrate, an observation confirmed in a separate reaction. After room temperature evaporation of the solvent and subsequent washing of the residue with pentane, only **3a** (¹H NMR) was present, with no detectable quantities of 2,5-dimethyltetrahydrofuran.

Aldehydes. Benzaldehyde, safranal, and *trans*-cinnamaldehyde were all tested for binding to **3a**, and, in all cases, they readily attach to the aggregate. Hence, when 6 equiv of benzaldehyde, *trans*-cinnamaldehyde, or safranal were added to **3a** dissolved in diethyl ether, the solution turned immediately bright yellow-orange. Slow evaporation of the solvent yielded crystalline residues in each case. Suitable single crystals can be grown for all of the complexes, and X-ray structural analysis was carried out for each. Figures 10, 11, and 12 depict the aggregates **3a**·6C₇H₆O·2C₆H₆·0.8C₅H₁₂ (benzaldehyde), **3a**·6C₉H₈O·¹/₂Et₂O (*trans*-cinnamaldehyde) and **3a**·6C₁₀H₁₄O·Et₂O

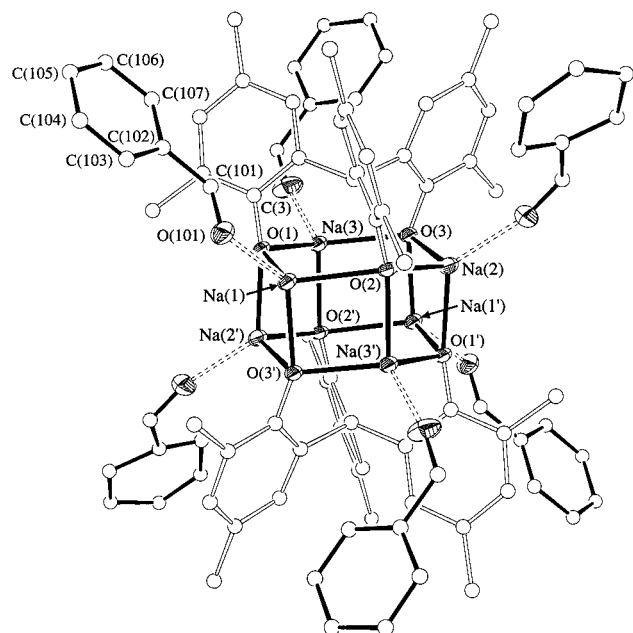


Figure 10. ORTEP (30% ellipsoids) representation of $3\mathbf{a}\cdot 6\text{C}_7\text{H}_6\text{O}\cdot 2\text{C}_6\text{H}_6\cdot 0.8\text{C}_5\text{H}_{12}$, with carbon atoms depicted as spheres. For clarity, the benzaldehyde molecules and the aggregate core have been drawn with solid lines. The numbering scheme follows that depicted in Figure 1. The solvent molecules have been omitted, together with the *tert*-butyl groups and hydrogen atoms. Only one of the benzaldehyde molecules has been numbered with the remaining two unique benzaldehyde molecules numbered analogously. The remainder of the structure, denoted by primed and unprimed atoms, is related by an inversion center.

(safranal), with selected bond lengths and angles shown in Table 5, and crystallographic parameters in Table 4.

Upon examination of the structures, it is immediately clear that all six binding sites are occupied by the respective aldehydes, although in the benzaldehyde system, two aldehyde molecules are significantly more distant (~ 0.13 Å) from the sodium atoms than the other four. Moreover, the Na–O–C angle of $109.4(3)^\circ$ for these two groups is clearly distinct from the others ($\sim 165^\circ$). Other than “crystal packing forces”, the cause of this inconsistency is not immediately apparent, since the Na–O distances and Na–O–C angles for the other similarly sized aldehyde systems are indistinguishable for all six sites. Moreover, in solution, the ^1H NMR exhibits sharp signals congruent with a C_3 -symmetric complex.

The substrate *trans*-cinnamaldehyde appears to be the weakest ligand for the sodium aggregate (besides the benzaldehyde outliers), since its bond lengths are on average 0.075 Å longer than for the other aldehydes. Despite these minor discrepancies, examination of the remaining parameters reveals that all three aldehyde structures are, in fact, remarkably similar, with the majority of the corresponding bond lengths and angles being comparable, and so a discussion of the individual structures is uninformative.

From a comparison of these structures with that of $3\mathbf{a}\cdot 6\text{THF}$, the aldehydes seem to be better ligands for the aggregates than THF. The Na–O bond lengths are, on average, 0.156 , 0.072 , and 0.138 Å shorter for benzaldehyde, *trans*-cinnamaldehyde, and safranal systems, respectively, than those in $3\mathbf{a}\cdot 6\text{THF}$. The *ipso*-carbon interactions are, however, significantly shorter (~ 0.12 Å) than those found in the THF system, which may be indicative of more electron deficient sodiums.

If these compounds are to be considered as Lewis acids, then, from a synthetic standpoint, the most important parameters

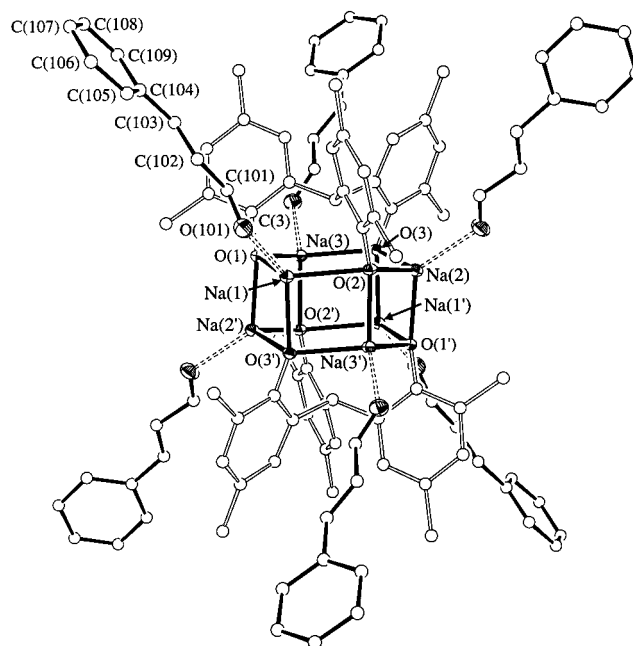


Figure 11. ORTEP (30% ellipsoids) representation of one of the two unique molecules in $3\mathbf{a}\cdot 6\text{C}_9\text{H}_8\text{O}\cdot \frac{1}{2}\text{Et}_2\text{O}$, with carbon atoms depicted as spheres. For clarity, the cinnamaldehyde molecules and the aggregate core have been drawn with solid lines. The numbering scheme follows that depicted in Figure 1. The solvent molecule has been omitted, together with the *tert*-butyl groups and hydrogen atoms. Only one of the cinnamaldehyde molecules has been numbered with the remaining cinnamaldehyde molecules numbered analogously. The remainder of the molecule, denoted by primed and unprimed atoms, is related by an inversion center. The other unique aggregate is numbered analogously but appended with “B”.

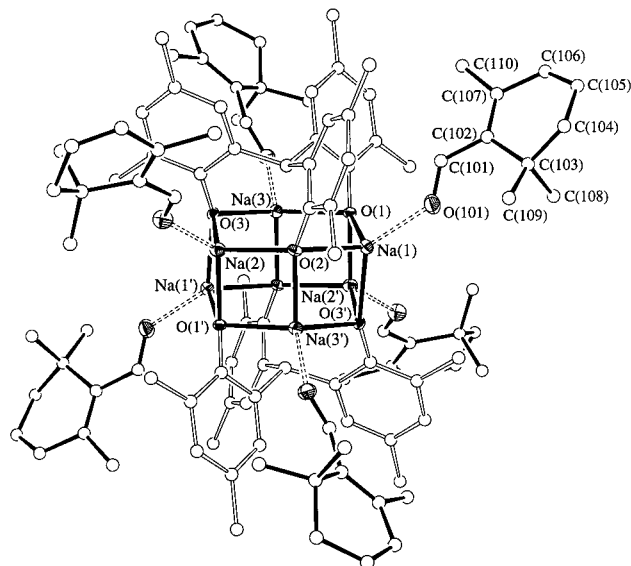


Figure 12. ORTEP (30% ellipsoids) representation of $3\mathbf{a}\cdot 6\text{C}_{10}\text{H}_{14}\text{O}\cdot \text{Et}_2\text{O}$, with carbon atoms depicted as spheres. For clarity, the safranal molecules and the aggregate core have been drawn with solid lines. The numbering scheme follows that depicted in Figure 1. The solvent molecule has been omitted, together with the *tert*-butyl groups and hydrogen atoms. Only one of the safranal molecules has been numbered, with the remaining two safranal molecules numbered analogously. The remainder of the structure, denoted by primed and unprimed atoms, is related by an inversion center.

would be those associated with substrate, particularly the carbonyl bonding distances, since significant lengthening in these bonds may infer their activation by the metal. Reliable data for other materials containing *trans*-cinnamaldehyde or

Table 5. Selected Bond Lengths (Å) and Angles (deg) for the Aldehyde Adducts of **3a**

	3a ·6C ₇ H ₆ O·2C ₆ H ₆ ·0.8C ₅ H ₁₂ (benzaldehyde)	3a ·6C ₉ H ₈ O·1/2Et ₂ O (<i>trans</i> -cinnamaldehyde)	3a ·6C ₁₀ H ₁₄ O·Et ₂ O (safranal)
Na(1)···O(101)	2.371(3)	2.326(3)	2.250(4)
Na(2)···O(201)	2.247(3)	2.320(3)	2.256(4)
Na(3)···O(301)	2.236(3)	2.328(2)	2.271(4)
Na(1)–O(1)	2.322(3)	2.307(2)	2.282(3)
Na(1)–O(2)	2.381(3)	2.407(2)	2.300(3)
Na(1)–O(3')	2.258(2)	2.271(2)	2.270(3)
Na(1)···C(17)	2.664(4)	2.651(3)	2.673(4)
Na(2)···C(31)	2.686(3)	2.674(3)	2.663(4)
Na(3)···C(3)	2.664(3)	2.666(3)	2.649(4)
O(101)–C(101)	1.209(5)	1.216(5)	1.227(6)
O(201)–C(201)	1.223(8)	1.211(4)	1.219(6)
O(301)–C(301)	1.190(6)	1.217(4)	1.210(6)
Σ[C _{ipso} –C(1)–C _{ipso}]	337.4(5)	336.9(3)	337.6(5)
Na(1)–O(101)–C(101)	109.4(3)	123.9(2)	129.1(3)
Na(2)–O(201)–C(201)	164.8(4)	120.7(2)	123.2(3)
Na(3)–O(301)–C(301)	165.3(4)	124.3(2)	121.2(3)
Na(1)–O(1)–Na(3)	126.6(1)	123.56(8)	125.0(1)
Na(1)–O(1)–Na(2')	85.13(8)	85.65(7)	83.8(1)
O(1)–Na(1)–O(2)	108.47(9)	111.04(8)	110.6(1)
O(1)–Na(1)–O(3')	96.32(9)	96.10(7)	97.8(1)
O(2)–Na(1)–O(3')	94.21(8)	92.65(7)	93.8(1)
O(1)–Na(1)–O(101)	103.3(1)	101.2(1)	100.8(1)
O(2)–Na(1)–O(101)	117.5(1)	118.42(9)	121.3(1)
O(3')–Na(1)–O(101)	131.5(1)	134.96(9)	130.1(1)

safranal are not available, although a number of structures containing benzaldehyde have been reported. For main group elements, four structures have been published; PhCHO···BF₃ [C=O 1.244(5) Å],³⁷ PhCHO···B(C₆F₅)₃ [C=O 1.241(7) Å],³⁸ [InCl₃(PhCHO)₃]₂ (average length 1.228 Å),³⁹ and Al(2,6-Ph₂C₆H₃)₃(PhCHO) (no data given or deposited).² For the transition metals with η¹-coordinated benzaldehyde, three examples have been reported: [Cp(CO)₃W(PhCHO)]⁺OTf[−] [C=O 1.216(9) Å],⁴⁰ TPPZn(PhCHO) (1.220 Å),⁴¹ and Ti(O^{*i*}-Pr)₃(PhCHO)(OEt₂) [1.224(1) Å].⁴² Bond lengths in the various transition metal complexes with benzaldehyde coordinated in a η²-fashion are not relevant to the current complex, although, unsurprisingly, much longer lengths are observed in these cases.⁴⁰ The indium and zinc structures also each contain an uncoordinated benzaldehyde in the crystal lattice (C=O bond length 1.218 and 1.213 Å, respectively) and represent the only structural characterizations of the free aldehyde. The carbonyl bond lengths measured in **3a**·6C₇H₆O, averaging 1.21 Å, are thus comparable to those in other metal complexes, but are probably not significantly activated relative to the boron systems.

Infrared and, to a lesser extent, ¹³C NMR spectroscopy are more useful measures of CO bond strength, and a complete summary of all relevant data for the starting material and products is given in Table 6. From this data, it is immediately clear that the carbonyl bond is not significantly activated with respect to the starting materials. Indeed, for the benzaldehyde system (and, to a lesser extent, for the acetophenone system, vide infra) a slight *increase* in wavenumber (8 cm^{−1}) is observed, possibly indicating an increase in bond strength. For the *trans*-cinnamaldehyde and safranal systems, although only

very modest, the expected decreases of 9 and 8 cm^{−1} were measured. Other systems containing η¹-coordinated benzaldehyde where IR data is given show stretch decreases of 84, 93, and 67 cm^{−1} for the B(C₆F₅)₃, tungsten, and titanium systems, respectively.

The ¹³C NMR data for the carbonyl carbon shows similar results. Relative to the starting materials, slight increases in the chemical shift of the carbonyl carbon of 2.4, 2.0, and 1.2 ppm for benzaldehyde, cinnamaldehyde, and safranal systems were observed, tentatively indicating a slight weakening of this bond. These compare with increases of 8.0 (BF₃), 7.3 [B(C₆F₅)₃], 22.7 (tungsten), and 9.2 ppm (titanium) for the other respective benzaldehyde complexes.

The resonance in the ¹H NMR arising from the aldehyde proton is also of particular interest, as it should shift markedly upon coordination if changes in its environment have occurred. For the three aldehydes, *upfield* differences of 0.77 (benzaldehyde), 0.66 (cinnamaldehyde), and 0.84 ppm (safranal) were recorded. These large changes are probably associated with shielding of the aldehyde proton from the magnetic field by the bulky ligand, rather than electronic changes, which, in light of the small carbonyl chemical shift differences, are almost insignificant. Supporting this notion, the titanium and tungsten systems exhibit *downfield* differences of 0.24 and 0.52 ppm, respectively.

Ketones. For the binding studies with ketones, both bulky and nonbulky systems were tested, namely, cyclohexyl methyl ketone, acetophenone, pivalophenone (α,α,α-trimethylacetophenone), 2,2,4,4-tetramethylpentan-2-one, *cis*- and *trans*-2,6-dimethylcyclohexanone, and 2,2,6-trimethylcyclohexane-1,4-dione. Unlike the benzaldehyde systems, when 6 equiv of cyclohexyl methyl ketone was added to an ether solution of **3a**, no color change occurred since this aliphatic ketone has no moiety capable of significant electron delocalization. The substrate is much bulkier than the aldehydes previously characterized, so a single-crystal X-ray structure was undertaken. The material has only limited solubility in ether, and single crystals of **3a**·6C₈H₁₄O form on standing after addition of the ketone. Like the dichloromethane adduct previously discussed,

(37) Reetz, M. T.; Hullmann, M.; Massa, W.; Berger, S.; Rademacher, P.; Heymanns, P. *J. Am. Chem. Soc.* **1986**, *108*, 2405.

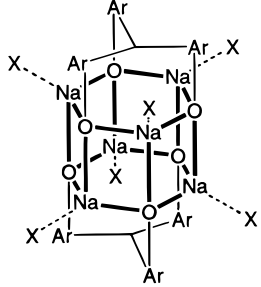
(38) Parks, D. J.; Piers, W. E. *J. Am. Chem. Soc.* **1996**, *118*, 9440.

(39) Jin, S.; McKee, V.; Nieuwenhuyzen, M.; Robinson, W. T.; Wilkins, C. J. *J. Chem. Soc., Dalton Trans.* **1993**, 3111.

(40) Song, J.-S.; Szalda, D. J.; Bullock, R. M. *Inorg. Chim. Acta* **1997**, *259*, 161.

(41) Byrn, M. P.; Curtis, C. J.; Hsiou, Y.; Khan, S. I.; Sawin, P. A.; Tendick, S. K.; Terzis, A.; Strouse, C. E. *J. Am. Chem. Soc.* **1993**, *115*, 9480.

(42) Gau, H.-M.; Lee, C.-S.; Lin, C.-C.; Jiang, M.-K.; Ho, Y.-C.; Kuo, C.-N. *J. Am. Chem. Soc.* **1996**, *118*, 2936.

Table 6. Comparison of Relevant Infrared and NMR^a Spectroscopic Data for Compounds **3a** and **3b** and Their Adducts


compound		IR ν CO (cm ⁻¹)		¹³ C NMR CO (ppm) ^a		¹³ C NMR	central methine (ppm) ^a	
salt	X	product	free substrate	product	free substrate	O-CAr (ppm) ^a	¹ H	¹³ C
3a						161.7	8.13	31.6
3b						161.1	7.76	33.2
3a	THF						8.24	
3b	THF					162.2	8.11	30.0
3b	CH ₂ Cl ₂						7.83	
3a	benzaldehyde	1712, 1696	1704, 1690	193.8	191.4	162.6	8.63	31.7
3a	<i>trans</i> -cinnamaldehyde	1672, 1626	1681, 1626	194.5	192.5	162.8	8.59	31.9
3a	safranal	1656, 1635	1664, 1634	192.1	190.9	162.5	8.44	31.6
3a	acetophenone	1692, 1601	1688, 1601	197.9	196.6	162.7	8.76	30.5
3a	pivalophenone	1671, 1602	1677, 1600	207.3	207.2	161.4	8.19	30.5
3a	cyclohexyl methyl ketone	1706	1710	212.3	209.1	162.4	8.48	28.9
3a	2,6-dimethylcyclohexanone	1713	1711		214.2		8.38	
3b	2,2,6-trimethylcyclohexan-1,4-dione	1721, 1712	1724, 1709	208.0	205.9	161.3	7.94	32.1

^a NMR spectra recorded in *d*₆-benzene at 299.95 and 75.47 MHz for the proton and carbon channels, respectively.

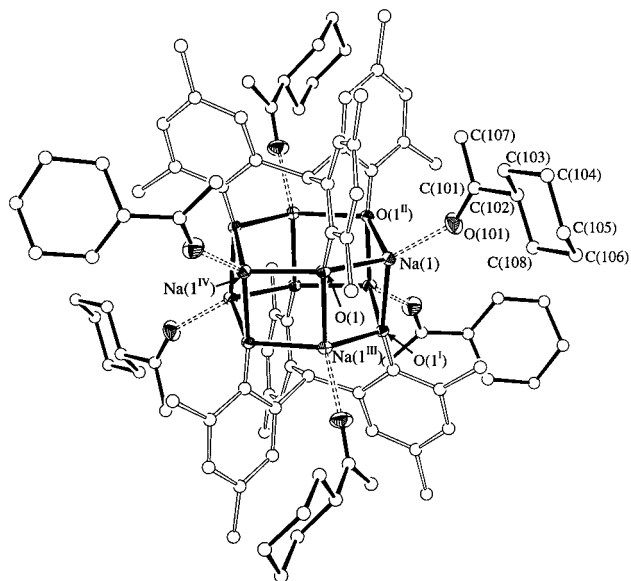


Figure 13. ORTEP representation of “Molecule 1” in **3b**·C₈H₁₄O (30% probability ellipsoids), with carbon atoms depicted as spheres. Both unique molecules in the asymmetric unit reside on *S*₆ symmetry positions, relating all of the sodium atoms, aromatic rings, and ketones. “Molecule 2” follows an analogous numbering scheme, appended with “B”. *tert*-Butyl methyl groups and hydrogen atoms have been omitted for clarity.

the compound crystallizes in the hexagonal space group *R* $\bar{3}$, with the central carbon residing on an *S*₆ symmetry axis, with only one aromatic ring, sodium, and coordinated ketone unique. Figure 13 depicts the structure, Table 6 gives the collection and refinement data, and selected bond lengths and angles are shown in Table 8.

As expected, the structure of this species is analogous to those previously characterized, with the carbonyl oxygen making a close approach to the sodium [2.239(2) Å]. To accommodate the ketone, a slight structural rearrangement in the aggregate

has taken place. The bond lengths in the aggregate core are, on average, shorter than those in the aldehyde examples, and the Na–C(17) *ipso*-carbon interaction, of 2.805(2) Å, is the longest yet seen, possibly due to the somewhat bulkier nature of this particular ketone. The other structural features are typical and have already been discussed.

Much like the aromatic aldehyde complexes, addition of acetophenone to a solution of **3a** induces a visible color change from colorless to bright yellow. Spectral and microanalytical data confirmed the expected association of six acetophenones per aggregate. When the more sterically encumbering acetophenone derivative pivalophenone was added to **3a**, no color change occurred. Initially, the absence of a perceptible color change was ascribed to the failure of the bulky substrate to bind to the sodiums, but NMR analysis dispelled this notion, since the spectrum indicated that four pivalophenones were associated per aggregate. Single crystals of the material were grown by diffusion of pentane in a saturated ether solution, and a structural analysis was undertaken. An ORTEP representation of the structure is shown in Figure 14. Collection parameters are shown in Table 7, with selected bond lengths and angles presented in Table 8.

Upon inspection of the structure, it is immediately apparent that the stoichiometry determined by NMR is correct, with four pivalophenones bound to sodiums, while the remaining two coordination sites are vacant. The vacant sites are each occupied by a molecule of diethyl ether, which, like four of those in **3a**·2Et₂O·2²/₃Et₂O discussed earlier, are in no way associated with the sodium atoms. In order to accommodate this extremely large ketone, a significant distortion in the aggregate core is required to open up the sodium sites, and even the ketone itself has had to twist away from an ideal configuration. The most significant deviations are clearly evident in the core, which has almost split apart. The distance between the sodium atoms associated with the ketones and the adjacent oxygen atoms has increased markedly, so much so that they really can no longer be considered bonded. The Na(1)–O(1) and Na(2)–O(3) distances,

Table 7. X-ray Data^a for the Crystal Structures of the Ketone Adducts of **3a**

	3a ·6C ₈ H ₁₄ O (cyclohexyl methyl ketone)	3a ·4C ₁₁ H ₁₄ O·2Et ₂ O (pivalophenone)	3a ·5.6C ₈ H ₁₄ O·0.9Et ₂ O (2,6-dimethyl- cyclohexanone)	<i>trans</i> -2,6-dimethylcyclo- hexanone 2,4-di- nitrophenylhydrazone	3a ·6C ₉ H ₁₄ O ₂ ·0.4Et ₂ O (2,2,6-trimethyl- cyclohexane-1,4-dione)
total reflns	38689	19913	67341	7183	45869
unique reflns	8712	13214	23140	2533	15676
collection range	1.11° < θ < 26.38°	1.82° < θ < 26.38°	0.82° < θ < 24.73°	1.42° < θ < 24.71°	1.62° < θ < 26.37°
T _{max,min}	1.00, 0.76	1.00, 0.93	1.00, 0.89	1.00, 0.79	1.00, 0.80
empirical formula	C ₁₃₄ H ₂₀₆ O ₁₂ Na ₆	C ₁₃₈ H ₁₉₈ O ₁₂ Na ₆	C _{134.4} H _{209.4} O _{12.5} Na ₆	C ₁₄ H ₁₈ N ₄ O ₄	C _{153.6} H ₂₃₄ O _{18.4} Na ₆
M _r	2146.93	2186.90	2163.16	306.32	1256.47
cryst syst	hexagonal	triclinic	monoclinic	monoclinic	monoclinic
space group	R $\bar{3}$	P $\bar{1}$	P2 ₁ /c	P2 ₁ /c	P2 ₁ /n
a (Å)	24.113(1)	14.380(1)	24.846(1)	15.609(4)	19.911(1)
b (Å)		16.048(1)	25.305(1)	6.877(2)	15.528(1)
c (Å)	37.981(2)	16.689(1)	21.591(1)	15.170(5)	24.873(2)
α (deg)		112.494(2)			
β (deg)		108.235(2)	91.816(1)	113.05(2)	91.051(1)
γ (deg)		95.270(2)			
V _c (Å ³)	19124(2)	3280.1(4)	13568(1)	1498.3(7)	7688.8(9)
D _c (g cm ⁻³)	1.118	1.107	1.098	1.358	1.085
Z	6	1	4	4	2
F(000)	7032	1188	4727	648	2738
μ(Mo Kα) (mm ⁻¹)	0.086	0.085	0.082	0.102	0.083
R1 [<i>I</i> ≥ 2σ(<i>I</i>) data] ^b	0.0552 [6382]	0.0606 [10293]	0.0968 [13916]	0.0444 [1539]	0.0746 [9656]
wR2 (all data); X, Y ^c	0.1660; 0.0798, 36.75	0.1482; 0.0466, 2.96	0.3336; 0.199, 7.46	0.1379; 0.0743, 0.00	0.2395; 0.1303, 4.64
GOF	1.020	1.068	1.113	1.017	1.029
largest peak, deepest trough (e Å ⁻³)	+0.88, -0.36	+0.85, -0.46	+1.59, -0.59	+0.25, -0.33	+0.84, -0.52

^a Obtained with monochromatic Mo Kα radiation (λ = 0.71073 Å). ^b R1 = Σ||F_o| - |F_c||/Σ|F_o|. ^c wR2 = {Σ[w(F_o² - F_c²)/Σ[w(F_o²)]}^{1/2} where w = 1/[σ²(F_o²) + (XP)² + YP] where P = (F_o² + 2F_c²)/3.

Table 8. Selected Bond Lengths (Å) and Angles (°) for the Ketone Adducts of **3a**

bond(s)	3a ·6C ₈ H ₁₄ O (cyclohexyl methyl ketone)	3a ·4C ₁₁ H ₁₄ O·Et ₂ O (pivalophenone)	3a ·5.6C ₈ H ₁₄ O·1/2Et ₂ O (2,6-dimethylcyclohexanone)	3b ·6C ₉ H ₁₄ O ₂ ·0.4Et ₂ O (2,2,6-trimethylcyclohexyl-1,4-dione)
Na(1)···O(101)	2.239(2)	2.434(2)	2.291(4)	2.282(3)
Na(2)···O(201)		2.394(2)	2.284(5)	2.275(3)
Na(3)···O(301)			2.309(4)	2.257(2)
Na(1)-O(1)	2.291(2)	2.316(2)	2.302(3)	2.293(2)
Na(1)-O(2)	2.332(2)	O(1 ^{II}) 2.588(2)	2.386(3)	2.363(2)
Na(1)-O(3')	2.275(1)	O(1 ^I) 2.319(2)	2.290(3)	2.261(2)
Na(1)···C(17)	2.805(2)	C(3 ^{II}) 2.678(2)	2.694(4)	2.724(3)
Na(2)···C(31)		2.651(2)	2.709(4)	2.775(3)
Na(3)···C(3)		2.612(2)	2.699(4)	2.748(3)
O(101)-C(101)	1.211(3)	1.225(3)	1.189(7)	1.226(4)
O(201)-C(201)		1.221(3)	1.130(9)	1.214(4)
O(301)-C(301)			1.178(7)	1.210(4)
Σ[C _{ipso} -C(1)-C _{ipso}]	338.7(1)	336.5(3)	337.2(5)	337.4(3)
Na(1)-O(101)-C(101)	151.1(2)	156.0(2)	176.4(4)	147.5(3)
Na(2)-O(201)-C(201)		152.6(2)	172.0(7)	175.5(2)
Na(3)-O(301)-C(301)			158.7(5)	159.9(3)
Na(1)-O(1)-Na(3)	124.70(6)	Na(1 ^{IV}) 123.82(6)	125.2(12)	122.66(9)
Na(1)-O(1)-Na(2')	84.94(5)	Na(1 ^{III}) 89.45(5)	86.7(1)	85.26(7)
O(1)-Na(1)-O(2)	112.15(6)	O(1 ^{II}) 106.99(5)	111.2(1)	111.04(8)
O(1)-Na(1)-O(3')	95.71(5)	O(1 ^I) 92.61(6)	94.9(1)	96.66(8)
O(2)-Na(1)-O(3')	94.60(5)	O(1 ^{II})/O(1 ^I) 88.35(5)	90.7(1)	94.75(7)
O(1)-Na(1)-O(101)	109.38(7)	119.06(7)	111.9(2)	115.9(1)
O(2)-Na(1)-O(101)	113.85(7)	O(1 ^{II}) 120.17(6)	118.2(2)	113.3(1)
O(3')-Na(1)-O(101)	129.42(7)	O(1 ^I) 123.02(7)	126.6(2)	122.5(1)

which in other structures are approximately 2.35 Å, have increased to 2.588(2) and 2.443(2) Å, respectively. Unlike the previous systems, this lengthening is not associated with the *ipso*-phenoxide carbon interactions and these distances are indistinguishable from the aldehyde coordinated sodium aggregates (~2.65 Å), although this contact would be expected to contribute additional stabilization. Furthermore, the steric bulk of the aggregate denies the pivalophenone molecules a close approach to the sodium atoms, and the Na-carbonyl distances are much longer (~0.15 Å) than those in the other clusters.

In addition to the distortions seen in the aggregate, the pivalophenone molecule itself can no longer adopt a planar geometry if it is to interact with sodium. This twist can be clearly

seen for the pivalophenone associated with Na(2) in Figure 14. Least-squares planes drawn through the aromatic rings, and the carbonyl groups and *ipso*-carbons exhibit considerable twists of 41.1° and 45.5° for the two unique pivalophenones bound to Na(1) and Na(2), respectively. This deformation explains the lack of color of this material, since π-delocalization between the carbonyl and aromatic ring is no longer possible.

Because this binding is most likely quite weak, we wondered if simple chemical separations of acetophenone and pivalophenone using **3a** were feasible. A stoichiometric mixture of the two ketones was added to a solution of **3a**, and the solution immediately turned yellow. Evaporation of the solvent and subsequent washing of the residue with pentane gave a yellow

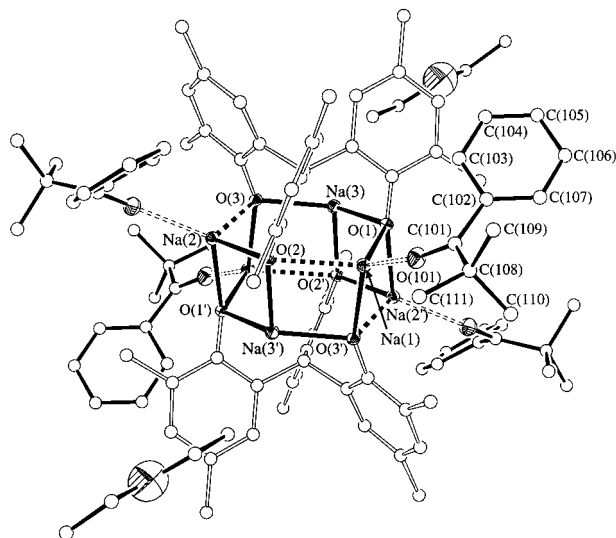
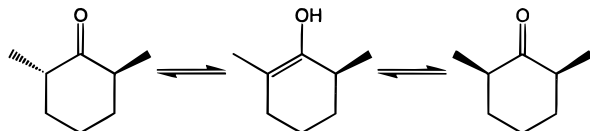


Figure 14. ORTEP (30% ellipsoids) representation of $3\mathbf{a}\cdot 6\text{C}_{11}\text{H}_{14}\text{O}\cdot \text{Et}_2\text{O}$, with carbon atoms depicted as spheres. For clarity, the pivalophenone molecules and the aggregate core have been drawn with solid lines. The numbering scheme follows that depicted in Figure 1. The *tert*-butyl groups and hydrogen atoms have been omitted. Only one of the pivalophenone molecules has been numbered, with the remaining pivalophenone molecule numbered analogously. The remainder of the structure, denoted by primed and unprimed atoms, is related by an inversion center.

solid, which was identified spectroscopically as the acetophenone adduct by comparison to an authentic sample of the material. Evaporation of the supernatant left a colorless oil, which was identified as pivalophenone. Although some losses of the bulkier ketone were noted, presumably due to evaporation, the measured yields of $\sim 70\%$ are respectable. Addition of aqueous HCl to the acetophenone adduct, after extraction with ether, gave a mixture of very pure acetophenone and $1\mathbf{a}$. Yamamoto et al. have achieved similar discrimination between these two ketones previously using MAD.¹³

The even bulkier ketone, 2,2,4,4-tetramethylpentan-2-one, fails to bind to $3\mathbf{a}$ to any extent. Thus, an ether solution containing both the ketone and $3\mathbf{a}$, after evaporation of the solvent and washing with pentane, gave only $3\mathbf{a}$, with the supernatant containing the tetramethylpentanone.

Scheme 2. Interconversion of *cis*- and *trans*-Dimethylcyclohexanone



To further investigate the utility of $3\mathbf{a}$ for chemical separations, the separation of the subtly different sized isomers of 2,6-dimethylcyclohexanone was attempted. Commercial 2,6-dimethylcyclohexanone is a thermodynamic mixture (Scheme 2) of *cis* and *trans* isomers,⁴³ which we determined by GC analysis to be in the ratio of 81.2:18.8 *cis*:*trans*.

An ether solution of $3\mathbf{a}$ was treated with a mixture of *cis*- and *trans*-2,6-dimethylcyclohexanone, in a stoichiometry that had at least 6 equiv of both isomers present. The solvent was slowly allowed to evaporate, depositing large crystals in the reaction flask, and these were carefully washed with pentane to remove any excess dimethylcyclohexanone. NMR and GC

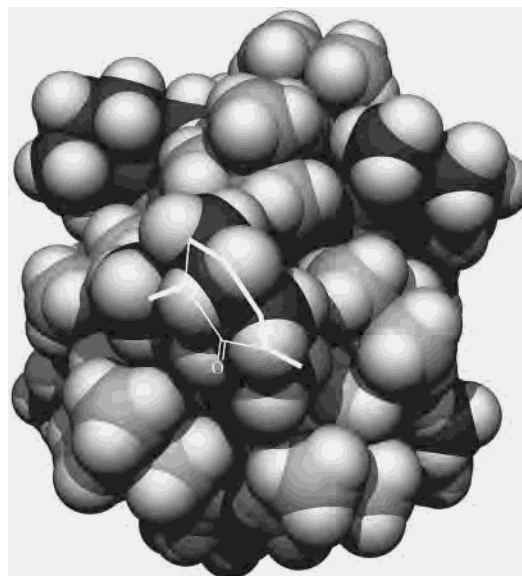


Figure 15. Space-filling representation of “molecule 1” of the structure of $3\mathbf{a}\cdot 5.6\text{C}_8\text{H}_{14}\text{O}$ (*trans*-2,6-dimethylcyclohexanone) for clarity, the 2,6-dimethylcyclohexanone carbons have been rendered darker than those of the triarylmethane units.

analysis (after addition of water) showed that the crystals still contained a mixture of *cis*- and *trans*-2,6-dimethylcyclohexanone, with approximately a 5:1 ratio, although now in favor of the *trans* isomer. An X-ray analysis was undertaken, although unfortunately an accurate determination was thwarted due to large amounts of disorder in the molecules. Repeated attempts were made to improve the structural information, and four complete data sets were collected, including one at -125°C . The latter data set was marginally better than the others, and it is the structure presented here. A space-filling representation is given in Figure 15, with collection parameters in Table 7, and selected bond lengths and angles given in Table 8, although these should be treated more cautiously than usual given the poor quality of the data.

The unit cell contains two unique molecules, both located on inversion centers, and so each represents half of an aggregate. The aggregate cores and triarylmethane moieties are, for the most part, well ordered, and the bulk of the disorder is associated with the ligating cyclohexanones. Nevertheless, in most cases, the geometry of the cyclohexanone could be deduced unambiguously, and in at least five out of six times, it is the *trans* isomer. Examination of Figure 15, where the cyclohexanone has been highlighted in dark, demonstrates the capacity of the *trans* isomer to fit almost perfectly into the “pocket”. The *cis* isomer would be expected to interfere to a greater degree with the *tert*-butyl groups, and this unfavorable interaction is, perhaps, the main cause of the selectivity in the binding event. In the structure, one complete aggregate contains only *trans* isomers, with other symmetry unique aggregates containing one severely disordered cyclohexanone molecule, possibly a position occupied to some extent by the *cis* isomer.

To demonstrate the utility of this material in organic synthesis, the 2,6-dimethylcyclohexanone complex was treated with 2,4-dinitrophenylhydrazine to give the corresponding hydrazone. After crystallization, NMR analysis confirmed that the product contained only one distinct isomer of the hydrazone. With the intention of unambiguously determining the absolute geometry, a single-crystal X-ray structure determination was also undertaken. Figure 16 shows an ORTEP representation of 2,6-dimethylcyclohexanone 2,4-dinitrophenylhydrazone, with se-

(43) D’Silva, T. D. J.; Ringold, H. J. *Tetrahedron Lett.* **1967**, 1505.

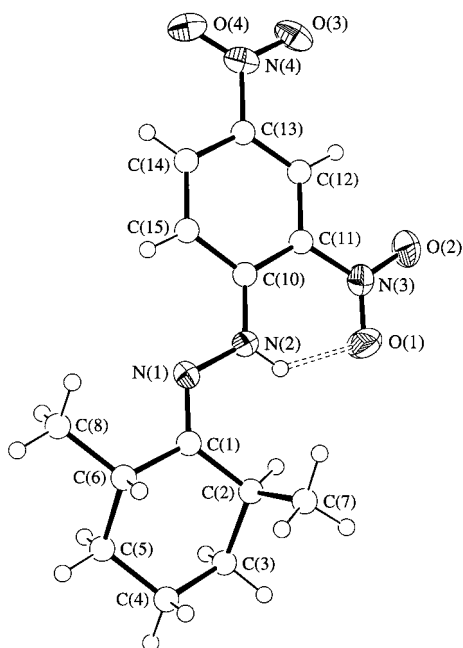


Figure 16. ORTEP representation (50% ellipsoids) of *trans*-2,6-dimethylcyclohexanone 2,4-dinitrophenylhydrazone, with carbon atoms depicted as spheres. Selected bond lengths (Å) and angles (deg) C(1)–N(1) 1.286(3), N(1)–N(2) 1.385(3), N(2)···O(1) 2.610(3), N(2)H···O(1), 1.959(3); C(1)–N(1)–N(2) 116.9(2), N(1)–N(2)–C(1) 119.9(2), N(2)–H–O(1) 131.6(2).

lected bond lengths given in the caption, and collection data in Table 6. The structure is itself, of course, unextraordinary, but it is immediately clear that only the *trans* isomer is present. The bond lengths and angles are typical, and the nitro groups lie in the aromatic plane as predicted. The hydrazone proton was located in difference maps and is hydrogen-bonded to the ortho nitro group, H···O 1.959(3) Å.

The final carbonyl ligand tested was the bifunctional ketone, 2,2,6-trimethylcyclohexane-1,4-dione. This ketone contains two carbonyl moieties, one in a sterically crowded environment, the other in an uncrowded environment. With this substrate, the sodium aggregate should selectively bind only to the unhindered site. Accordingly, when 6 equiv of 2,2,6-trimethylcyclohexane-1,4-dione was added to a solution of **3b**, large colorless cubes formed on standing. The material has only very low solubility in common noncoordinating solvents, but ^1H and ^{13}C NMR spectra could be acquired, although an explicit determination of the binding orientation cannot be deduced from this data. For this reason, a structural determination was also undertaken. Figure 17 exhibits an ORTEP of the structure, with selected bond lengths and angles contained in Table 8, while Table 7 presents the collection details. In this structure, the expected binding orientation of the ketone on the sodiums is present in all six cases. The 2-carbonyl and its immediate environment is clearly a good match for the “pocket” in **3b**, and bond lengths and angles are typical compared with the other systems showing favorable binding already discussed.

The Na–O–C angles of the coordinated ketones would be expected to become more linear as the steric bulk around the carbonyl is increased. Of course, the average of the angles must be compared, since slight conformational changes permitting enhanced binding of one ketone may well be at the expense of another. Additionally, this angle is likely to be highly influenced by crystal packing forces. The variability of the Na–O–C angle is illustrated by the wide range of angles adopted by the 2,2,6-trimethylcyclohexane-1,4-dione adduct. An examination of the

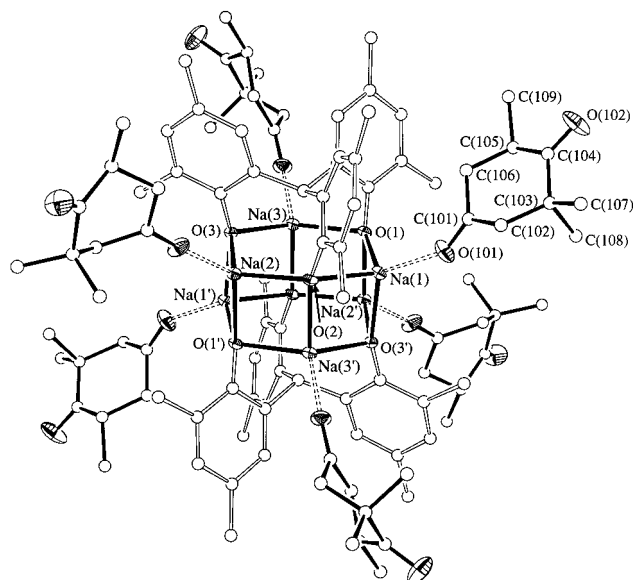


Figure 17. ORTEP (30% ellipsoids) representation of **3a**·6C₉H₁₄O₂·Et₂O, with carbon atoms depicted as spheres. For clarity, the 2,2,6-trimethylcyclohexane-1,4-dione molecules and the aggregate core have been drawn with solid lines. The numbering scheme follows that depicted in Figure 1. The amyl methyl groups and hydrogen atoms have been omitted. Only one of the 2,2,6-trimethylcyclohexane-1,4-dione molecules has been numbered, with the remaining 2,2,6-trimethylcyclohexane-1,4-dione molecules numbered analogously. The remainder of the structure, denoted by primed and unprimed atoms, is related by an inversion center.

angles for the ketone derivatives does tentatively suggest that a trend exists. Unfortunately, the bulkiest ketone, pivalophenone, cannot be directly compared since only four are bound, greatly affecting the structure. The remaining three, in order of decreasing steric requirement, are 2,6-dimethylcyclohexanone, 2,2,6-trimethylcyclohexane-1,4-dione, and cyclohexyl methyl ketone, showing average Na–O–C angles of 169.0°, 161.0°, and 151.1(2)°.

The pyramidalities of the sodiums with coordinated ketones and aldehydes are all very similar, as predicted, each being ~1.05 Å above the plane defined by their respective three phenoxide oxygens, with the exception of the pivalophenone derivative. For this compound the two unique sodiums with coordinated ketones [Na(1) and Na(2)] reside 1.22 and 1.16 Å above their oxo planes, while the remaining coordinatively unsaturated sodium is only 0.87 Å above its oxygen plane. These figures represent both extremes for all of the sodium salt adducts.

An obvious application for materials of this type would be for the selective derivatization of less reactive functional groups, since the more reactive site would be effectively protected due to the extremely steric environment around the sodium. We attempted a number of reactions of this type with **3b**·6C₉H₁₄O₂, including alkylations with methylmagnesium bromide and methyllithium and reductions with diisobutylaluminum hydride. These reactions were bedeviled by the extremely low solubility of **3b**·6C₉H₁₄O₂ in noncoordinating solvents such as diethyl ether, toluene or dichloromethane, especially at the low temperatures required for selective chemistry by these reagents.³ Workup of the reactions after addition of water at –78 °C yields only the starting dione, while warming of the reactions gives little to no selectivity. We surmise that reactions of this type may be successful if more soluble salts were synthesized or if the substrate imparted beneficial solubility characteristics to the adduct.

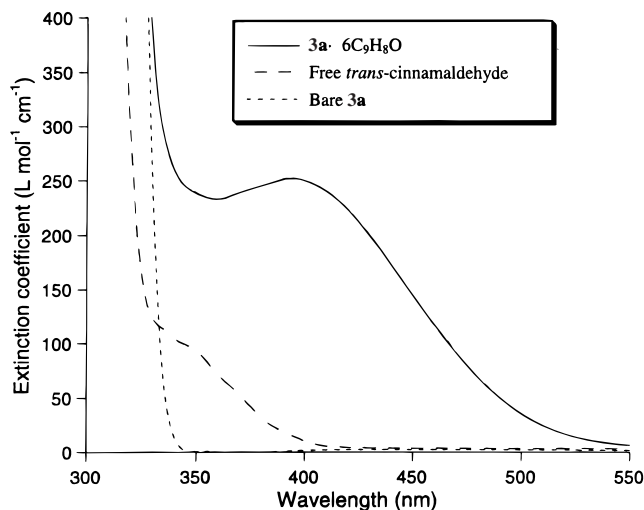


Figure 18. UV–visible spectrum of $3a \cdot 6C_9H_8O$, together with those of free $3a$ and *trans*-cinnamaldehyde in diethyl ether. The extinction coefficients are calculated per sodium and *trans*-cinnamaldehyde.

The general trends witnessed in the spectroscopic data of the aldehyde systems are also evident in the ketone complexes, and the data is tabulated in Table 6. In comparison to the large IR shifts witnessed in species such as MAD,^{3b} the strength of the ketone C=O bond is not affected significantly by coordination to the sodium, suggesting weak Lewis acidity of the aggregates. As seen for the benzaldehyde complex, a slight increase is seen in the infrared C=O stretch of the adduct between $3b$ and acetophenone, possibly suggesting a very minor increase in C=O bond strength.

The position of the central methine resonance in the 1H and ^{13}C NMR spectra indicates a significant variation for the adducts compared to uncoordinated 3 . Addition of a ketone produces a downfield shift of ~ 0.2 – 0.6 ppm (maximum for acetophenone and minimum for pivalophenone), signifying that its position is a tentative indicator for binding affinities, although no clear trend is evident. Like the aldehyde systems, the carbonyl resonances all show the expected downfield shift in the adducts with respect to the free ketones. In contrast, the shift is only very small (0.1 ppm) for pivalophenone, suggesting that in solution it is probably bound only to a negligible extent.

UV–Vis Spectra. For the aromatic aldehydes and ketones (with the exception of pivalophenone for reasons already discussed), a color change from colorless to bright-yellow orange occurred upon addition to solutions of $3a$. The UV–vis spectrum of free *trans*-cinnamaldehyde together with that of the $3a$ adduct, in the same relative concentrations, is presented in Figure 18. The free salt, $3a$, does not absorb in the visible region, and free *trans*-cinnamaldehyde absorbs only negligibly in this area. Upon coordination, the absorption maximum shifts significantly into the visible region of the spectrum. A similar result was measured for the benzaldehyde system, but unfortunately, both the acetophenone and safranal adducts exhibit very broad absorption ranges, and no maxima could be measured. This data could conceivably be used to quantify the binding affinities of

substrates toward $3a$ for substances that do not invoke absorbance(s) in this region, although studies to this effect have not been undertaken.

Reaction of $2a$ and $3a$ with Transition Metal Halides. The lithium and sodium salts of $1a$ should also have the potential to serve as precursors for the synthesis of transition metal derivatives.⁴⁴ A number of transition metal compounds were tested, including $TiCl_4$, $NbCl_5$, and $TaCl_5$, and all react immediately with $2a$ and $3a$, becoming dark orange. Unfortunately, the reactions do not proceed smoothly, and multiple and/or decomposition products were observed in all cases. Reactions were also attempted initially at -78 °C, followed by slow warming to room temperature, with similar results. The dimeric structure and steric constraints of $2a$ and $3a$ apparently prevent a favorable approach of the metal halide, complicating these reactions. To date, these materials have not been found to be useful precursors for further metal derivatization.

Conclusions

The lithium, sodium, and potassium salts of tris(3,5-dialkyl-2-hydroxyphenyl)methanes have been successfully synthesized and fully characterized, and, in all cases, these compounds form metal aggregates. The compounds feature well-defined, fairly stable structures that remain intact in a variety of solvents. For the sodium salts, coordinating solvent can be removed under vacuum, to leave coordinatively unsaturated sodium centers of defined size and shape. It should be possible to easily tune these “pockets” by synthesizing tris(3,5-dialkyl-2-hydroxyphenyl)methane derivatives incorporating different alkyl groups, including chiral ones. A number of oxygen donor compounds were found to readily bind to the sodiums, and in the case of acetophenone/pivalophenone, *cis/trans*-2,6-trimethylcyclohexanone, and 2,2,6-trimethylcyclohexane-1,4-dione, selective binding was observed. Thus, simple chemical separations can be carried out, as well steric protection of reactive carbonyl groups. Unfortunately, the present compounds are only poor Lewis acids, and metal activation or catalytic reactions with the present systems are not yet feasible. Nevertheless, incorporation of different metal aggregates into the tris(3,5-dialkyl-2-hydroxyphenyl)methane framework may afford reactive species and, efforts to prepare these complexes are currently underway.

Acknowledgment. We thank the University of Florida, the National Science Foundation (CAREER Award 9874966), and the donors of the American Chemical Society Petroleum Research Fund, for funding this research. Support from the Research Corporation is also gratefully acknowledged. We also express our gratitude to Dr. Khalil Abboud at the University of Florida for granting access to X-ray instrumentation and Prof. D. E. Richardson for providing a beta copy of MolPOV 2.

Supporting Information Available: Tables listing detailed crystallographic data, atomic positions, parameters, and bond lengths and angles. This material is available free of charge via the Internet at <http://pubs.acs.org>.

IC991309Q

(44) Special thematic issues on metal-aryloxide and alkoxide complexes; (a) *Polyhedron* **1995**, *14*, 3175. (b) *Polyhedron* **1998**, *17*, 623.